Macrozooplankton Abundances on the Scotian Shelf Using Acoustic Backscatter and Direct Sampling Methodologies

N.A. Cochrane, D.D. Sameoto, and M.K. Kennedy

Department of Fisheries & Oceans
Maritimes Region
Bedford Institute of Oceanography
PO Box 1006
Dartmouth, NS
B2Y 4A2

2017

Canadian Technical Report of Fisheries and Aquatic Sciences 3238

Fisheries and Oceans Canada | Pêches et Océans Canada

Canada

Canadian Technical Report of Fisheries and Aquatic Sciences

Technical reports contain scientific and technical information that contributes to existing knowledge but which is not normally appropriate for primary literature. Technical reports are directed primarily toward a worldwide audience and have an international distribution. No restriction is placed on subject matter and the series reflects the broad interests and policies of Fisheries and Oceans Canada, namely, fisheries and aquatic sciences.

Technical reports may be cited as full publications. The correct citation appears above the abstract of each report. Each report is abstracted in the data base *Aquatic Sciences and Fisheries Abstracts*.

Technical reports are produced regionally but are numbered nationally. Requests for individual reports will be filled by the issuing establishment listed on the front cover and title page.

Numbers 1-456 in this series were issued as Technical Reports of the Fisheries Research Board of Canada. Numbers 457-714 were issued as Department of the Environment, Fisheries and Marine Service, Research and Development Directorate Technical Reports. Numbers 715-924 were issued as Department of Fisheries and Environment, Fisheries and Marine Service Technical Reports. The current series name was changed with report number 925.

Rapport technique canadien des sciences halieutiques et aquatiques

Les rapports techniques contiennent des renseignements scientifiques et techniques qui constituent une contribution aux connaissances actuelles, mais qui ne sont pas normalement appropriés pour la publication dans un journal scientifique. Les rapports techniques sont destinés essentiellement à un public international et ils sont distribués à cet échelon. II n'y a aucune restriction quant au sujet; de fait, la série reflète la vaste gamme des intérêts et des politiques de Pêches et Océans Canada, c'est-à-dire les sciences halieutiques et aquatiques.

Les rapports techniques peuvent être cités comme des publications à part entière. Le titre exact figure au-dessus du résumé de chaque rapport. Les rapports techniques sont résumés dans la base de données *Résumés des sciences aquatiques et halieutiques.*

Les rapports techniques sont produits à l'échelon régional, mais numérotés à l'échelon national. Les demandes de rapports seront satisfaites par l'établissement auteur dont le nom figure sur la couverture et la page du titre.

Les numéros 1 à 456 de cette série ont été publiés à titre de Rapports techniques de l'Office des recherches sur les pêcheries du Canada. Les numéros 457 à 714 sont parus à titre de Rapports techniques de la Direction générale de la recherche et du développement, Service des pêches et de la mer, ministère de l'Environnement. Les numéros 715 à 924 ont été publiés à titre de Rapports techniques du Service des pêches et de la mer, ministère des Pêches et de l'Environnement. Le nom actuel de la série a été établi lors de la parution du numéro 925.

Canadian Technical Report of
Fisheries and Aquatic Sciences 3238

2017

MACROZOOPLANKTON ABUNDANCES ON THE SCOTIAN SHELF USING ACOUSTIC BACKSCATTER AND DIRECT SAMPLING METHODOLOGIES

by

N. A. Cochrane[1], D. D. Sameoto[2], and M. K. Kennedy[2]

[1]Ocean and Ecosystem Sciences Division
[2]Retired, formerly of
Ocean Sciences Division

Department of Fisheries & Oceans
Maritimes Region
Bedford Institute of Oceanography (BIO)
PO Box 1006
Dartmouth, NS
B2Y 4A2

Cat. No. Fs97-6/3238E-PDF ISBN 978-0-660-23611-7 ISSN 1488-5379

Correct citation for this publication:

Cochrane, N.A., Sameoto, D.D. and Kennedy, M.K. 2017. Macrozooplankton abundances on the Scotian Shelf using acoustic backscatter and direct sampling methodologies. Can. Tech. Rep. Fish. Aquat. Sci. 3238: viii + 66 p.

TABLE OF CONTENTS

LIST OF FIGURES

ABSTRACT

Cochrane, N.A., Sameoto, D.D. and Kennedy, M.K. 2017. Macrozooplankton abundances on the Scotian Shelf using acoustic backscatter and direct sampling methodologies. Can. Tech. Rep. Fish. Aquat. Sci. 3238: viii + 66 p.

Quantitative measures of Nova Scotian Shelf macrozooplankton abundance, dominated by the euphausiid *Meganyctiphanes norvegica*, were examined for the period 1961 – 2011. Main results included: 1) Echosounder and Acoustic Doppler Current Profiler (ADCP) backscatter abundances in Emerald Basin generally rising from the mid-1980s, peaking in 1994-95, while continuing to rise on the broader eastern and western shelf areas prior to a widespread, multi-year population crash in fall 2001. 2) Continuous Plankton Recorder (CPR) evidence of a long-term dip in larval euphausiid abundances the late 1990s. 3) Ring net and BIONESS multi-net euphausiid abundances sufficiently sparse and scattered to preclude long term trend delineation 4) Suggestive positive correlations between Emerald Basin column backscatter and both deep Basin temperatures and the North Atlantic Oscillation index. An extended discussion of acoustic methodologies is included. Avenues for further investigation are proposed.

RÉSUMÉ

Cochrane, N.A., Sameoto, D.D. and Kennedy, M.K. 2017. Abondance de macrozooplancton sur le plateau néo-écossais relevée à l'aide de méthodes de rétrodiffusion acoustique et d'échantillonnage direct. Rapp. tech. can. sci. halieut. aquat. 3238: viii + 66 p.

Les mesures quantitatives de l'abondance du macrozooplancton sur le plateau néo-écossais, dominée par les euphausiacés *(Meganyctiphanes norvegica*), ont été examinées pour la période de 1961 à 2011. Les principaux résultats comprennent : 1) Mesurées par l'échosondeur et la rétrodiffusion du profileur de courant à effet Doppler (ADCP), les abondances dans le bassin d'Émeraude sont en général à la hausse à partir du milieu des années 1980, atteignent un sommet en 1994-1995, tout en continuant à augmenter dans l'ensemble des zones est et ouest du plateau, avant l'effondrement pluriannuel généralisé de la population à l'automne 2001. 2) La preuve sur enregistreur continu de plancton (ECP) d'un déclin à long terme de l'abondance des euphausiacés larvaires vers la fin des années 1990. 3) Les abondances sont suffisamment rares et dispersées des euphausiacés dans les bolinches et le système d'échantillonnage à filets multiples BIONESS pour empêcher la délimitation des tendances à long terme. 4) Les corrélations positives sont plausibles entre les données de rétrodiffusion de colonne du bassin d'Émeraude et à la fois les températures en profondeur du bassin et l'indice d'oscillation nord-atlantique. Un examen approfondi des méthodes acoustiques est inclus. Des voies de recherche d'enquête supplémentaires sont proposées.

PREFACE

The present document is a compilation of research results from studies, many performed prior to 2007, with some more recent interpretation. The scarcity of systematic Scotian Shelf macrozooplankton abundance data especially for the two decades commencing in the mid-1980s contemporaneous with profound changes in Scotian Shelf ground fish abundances, dictated a special initiative to organize and to publish relevant materials still in our possession along with the associated interpretative thinking before staff retirements rendered it inaccessible to future researchers. Many early analyses including that of the **C**ontinuous **P**lankton **R**ecorder (CPR), net sampling, and ADCP backscatter had been preserved in graphical form only, frequently with fewer details regarding data selection and processing than desired. Nevertheless, the core information appeared intact. Some relevant field studies continued post-2007, particularly ongoing measures of 200 kHz acoustic backscatter in Emerald Basin until 2011, for which full documentation still exists, and for which the current report appeared the appropriate forum. Consequently, some net-sampled macrozooplankton data, and Scotian Shelf backscatter time series are reported for the first time. Later report sections addressing environmental correlations are of more recent construct and incorporate more up-to-date materials.

The intervening time has permitted reflection on earlier results and interpretations. Factors bearing on the accuracy of the DataSonics-based 200 kHz backscatter measurements (1980s technology) are now better understood. While further analyses of the DataSonics data from the broader Shelf are still possible, the presented daytime backscatter data from central Emerald Basin constitute the virtual total sum of easily interpretable backscatter data from that well-studied Scotian Shelf location. The 200 kHz time series were processed directly from the original DataSonics sounder database using custom in-house software. Transducer sensitivity, acoustic absorption, and system noise level corrections were applied in such a manner as to ensure both accuracy as well as methodological and presentational compatibility with earlier published pre-November 1996 backscatter results. Since 2006, with support from the National Acoustic Data Archive project, the entire Scotian Shelf DataSonics sounder-acquired multi-frequency backscatter database has been geo-referenced and converted to HAC (**H**ydro**Ac**oustics) standard acoustic interchange format – as footnoted in the report. These later conversions intentionally omitted critical temperature and absorption corrections which were impractical to research and to apply in total for the much larger database. While the overall quality of the DataSonics sounder data is considerably inferior to that possible with modern scientific sounding systems, the extended database still retains potential for future studies of long-term backscatter variations over wider regions of the Scotian Shelf/Slope than Emerald Basin - provided effort is expended to research the necessary additional corrections. A discussion of acoustic processing techniques has been included which exceeds the scope strictly required for the results of this report. This information may prove useful for future researchers making use of the wider acoustic database or attempting to harmonize new backscatter observations with old.

October 2017 N.A. Cochrane, D.D. Sameoto, and M.K. Kennedy

1. INTRODUCTION

Macrozooplankton, defined as organisms greater than 10 mm in length, are the least well studied group in the zooplankton community on the Scotian Shelf. The reasons for this are their rarity compared to the smaller zooplankton and their active mobility making their routine net capture difficult. Their distribution is also frequently patchy and unpredictable. On the Scotian Shelf, the dominant macrozooplankton are euphausiids representing about 35% of the total individuals from 200 taxa of macrozooplankton collected. Twelve species of euphausiids are present on the shelf and slope with *Meganyctiphanes norvegica* making up 31% of the 13 euphausiid species collected. The chaetognaths represent the second largest percentage, about 28% of the individuals collected; however, their biomass is much lower than that of euphausiids. The third important invertebrate group are the amphipods that make up about 6% of the total macrozooplankton numbers. Fish larvae represent about 7% of the organisms collected.

The Nova Scotian Shelf contains several basins > 200 m deep which represent about 5% of the total shelf area. These basins are biologically unique regions because they are the only areas of the shelf that contain large populations of the copepod *Calanus finmarchicus* and the euphausiid *Meganyctiphanes norvegica* at depths below 200 m during the entire year. Basin euphausiid populations are dominated by *M. norvegica*, a permanently resident species and a strong diel vertical migrator through all seasons. During daylight hours, most of the adult population is found below 150 m in the central portions of these Basins with, however, a small residual population in the upper 50 m. At night, most euphausiids migrate to the upper 75 m often with concentrations increasing towards the surface with a large fraction of the population in the upper 25 m (Cochrane et al. 1994; Sameoto et al. 1985, 1993). In the basins, columnar concentrations (m^{-2}) of both *M. norvegica* and *C. finmarchicus* are orders of magnitude higher than those found on the banks (Sameoto and Herman 1990). The high basin concentrations of copepods and euphausiids make these regions favourable feeding areas for fish and marine mammals that depend on zooplankton and macrozooplankton for prey. While basins are distributed along the entire length of the shelf, the largest, Emerald and LaHave, are found in the central shelf (Fig. 1). Basins of the central and western shelf are characterized by warmer ($\geq 5^{\circ}$ C) bottom temperatures than for the smaller basins characteristic of the eastern shelf. Annual biological surveys have indicated that the concentrations of euphausiids are generally higher in the central shelf basins than in the colder basins of the eastern shelf (Sameoto and Cochrane 1996; Sameoto et al. 1997, 1998). *C. finmarchicus* concentrations below 200 m start to increase during May after the first spring generation of this species matures to copepodite V stage. Copepod concentrations in the deep central shelf basins continue to increase with succeeding generations until October, when most of the overwintering shelf population of *C. finmarchicus* has completed its seasonal vertical migration into deep water (Sameoto and Herman 1990; Herman et al. 1991).

To better understand the geographic and temporal distribution of euphausiids on the Scotian Shelf, we have analysed acoustic backscatter data collected with both conventional

ship-mounted echosounders and an acoustic Doppler current profiler (ADCP) to supplement biological data collected from a variety of net samplers. This report considers Scotian Shelf acoustic backscatter data collected during the "spring" (April to June, commonly in April) and "fall" (September to November, commonly in October) seasons between years 1984 to 2011 inclusive in Emerald Basin together with broader shelf backscatter acquired from 1993 to the summer of 2005 inclusive. The textual term "survey" is used to delineate the individual scientific data collection cruises and does not imply the steaming of intensive close-spaced grid patterns often characteristic of fisheries acoustics surveys. Much acoustic data were collected opportunistically along transects between biological sampling stations, all depth ranges being sampled from the surface to 300 m on the shelf and slope.

A number of Scotian Shelf marine ecological studies and compilations have characterized the time interval spanned by our studies as one of profound biological change (Choi et al. 2005; Zwanenburg et al. 2006; Worcester and Parker 2010). In particular, the eastern Scotian Shelf ecosystem in the words of Choi et al. (2005) "…has changed status…from a community dominated by large-bodied demersal fish to one dominated by small demersal and pelagic fish species and benthic macro-invertebrates". This change largely occurred from the mid-1980s to the early 1990s. Absent from these discussions has been a thorough treatment of Scotian Shelf macrozooplankton. This report, by presenting macrozooplankton abundance measures, some of which have received limited or no exposure to date, attempts, in part, to fill the gap. Analytical thinking dating largely from this earlier era is outlined and, in select instances, is informed by more recent research findings.

2. METHODS

2.1. GENERAL

The following discussion of methodologies, especially acoustical, is broader than strictly required for the results presented. The intent is to place the reported acoustical work in the context of our overall backscatter acoustics program and to provide better understanding of earlier era analytical approaches for those wishing to extend this work using existing or future databases.

2.2. MULTI-FREQUENCY ECHOSOUNDER

2.2.1. Instrumentation

The multi-frequency echosounding system consisted of two dual-channel vertical beam DataSonics DFT-210 Environmental Echosounders. While the sounder technology was dated by the mid-1980s, its continued use with some modifications until 2011 maintained reasonable uniformity in sounder hardware, transducer types, and associated calibration methodologies spanning nearly three decades. Although analytical techniques continuously evolved, a high degree of continuity was maintained in basic analytical

approaches and core software components allowing data collected over the entire sampling period to be compared in a compatible manner.

Prior to spring 1997, four acoustic transducers were simultaneously excited at 12, 50, 122, and 200 kHz. The 12 kHz transducer was hull-mounted while the others were mounted in a shallow towed acoustic fish. Table 1 specifies the most commonly utilized sounder operational parameters[1].

From the spring of 1997 onwards, operation was restricted to two frequencies: 200 kHz and 12 kHz. The 200 kHz transducer was deployed in a removable hull-mount on *CCGS Hudson*. The 12 kHz transducer was semi-permanently ram-mounted and during operation lowered about 1 m below the hull. The current report limits itself to quantitative results using the 200 kHz transducer.

The 200 kHz 200B-8 Furuno transducers, critical to this study, have been recalibrated several times using an in-lab surface planar reflection technique. During calibration the transducers were mounted either internally in the tow fish body or freely exposed to the water as appropriate to the at-sea collections. The 50, 122 and 200 kHz transducers possessed sufficient temperature coefficients in their combined transmit/receive sensitivities (Sameoto et al. 1993) that considering the full range of Scotian Shelf near-surface water temperatures these thermal characteristics had to be quantitatively measured over a comparable temperature range during calibration. Precise temperature control of the acoustic calibration tank was achieved by use of water refrigeration units. No clear systematic changes in DataSonics system transducer sensitivities over time **at fixed temperatures** have been detected. Since 1997, the 12 kHz transducer has been exchanged several times and in-situ biological fouling effects have occasionally been suspected. Consequently, the more recent 12 kHz backscatter data (used in this report to guide 200 kHz data selection only) should be considered uncalibrated. Neither the more recently used 200 kHz Furuno hull-mounted transducer nor the earlier towed 50, 122, and 200 kHz transducers were immersed for sufficient durations for bio-fouling to create calibration uncertainty.

To achieve adequate signal-to-noise ratios to permit quantification of scattering layers beyond 250 m depth at 200 kHz, a 5 ms transmit pulse length was normally used in combination with a 1 kHz sounder pass-band (narrowest selectable bandwidth). Nominal peak power output was about 2 kW, close to the transducer cavitation limit. This has raised concerns about possible non-linear acoustic propagation losses, an effect not appreciated during the earlier periods of usage (Tichy et al. 2003). It is uncertain if non-linear propagation effects did significantly influence the quantitative accuracy of our subsequent analyses. Such effects might account for the much higher than anticipated dependence of combined transducer transmit/receive sensitivity on transducer temperature. The strongest non-linear effects would be expected to occur within the water path immediately adjacent

[1] Reference is made to the wider DataSonics echosounder multiple-frequency acoustic database which is available for future analysis. The current report presents quantitative results from the 200 kHz channel only although other channels, especially 12 kHz, were regularly used during analysis to place appropriate depth bounds for assessing euphausiid column backscatter.

to the transducer face. Any non-linear effects would be partially removed (probably about one half of the total) by the system calibration procedures employed. Our best estimate is that residual non-linear effects could result in an up to a 2 dB systematic underestimate of true 200 kHz backscatter levels at typical euphausiid observation ranges of about 250 m. Since daytime euphausiid backscatter in Emerald Basin was typically confined to narrow depth intervals at long ranges from the transducer, **relative** backscatter levels viewed over time might be expected to be less affected than **absolute** backscatter levels. More conservative sounder power levels (Table 1) proved adequate at 12 kHz to reveal fish aggregations at the ≤ 300 m depths of interest in euphausiid studies. Hardware-based time variable gain (TVG) of 20 log R + 2αR decibel form, R being the measurement range from the transducer, was applied to all channels at **fixed** predefined rates. Sounder dynamic range limitations restricted real-time hardware-applied TVG corrections to profiling ranges of 2 – 200 m for the 121 and 200 kHz channels. More precise TVG absorption corrections extending to the maximum profiled depth range were applied in software during subsequent analysis as described below.

The demodulated sounder outputs were low-pass filtered at 1 kHz then digitized (custom in-house constructed digitizer) at 5 kHz/channel to 12 bit resolution and logged to a storage device. Time and date from 1987 onwards; together with GPS position, GPS course and speed, vessel gyro heading and vessel log speed from 1996 onwards; were incorporated into logged individual ping data headers at acquisition time[2].

2.2.2. Sampling Methodologies

The multi-frequency sounders were commonly pinged at 2 s intervals (this rate was varied for specific objectives) to provide real-time, close-spaced bathymetric soundings to control the deployment depths of simultaneously towed instrumentation. On shelf-wide transects the sounder data stream was decimated by a factor of 5 and logged at 1 ping/10 s. For shorter transects, often in conjunction with station net sampling, backscatter data were frequently logged at the full 1 ping/2 s rate. During many post 1997 surveys, the acoustic sounders were operated continuously and autonomously for the entire duration (up to two weeks) at an invariant 1 ping/10 s rate with data logged at the same rate. The most common post-ping sampling duration was 409 ms, which employing a 7 m transducer draft yielded a maximum profiling depth of about 310 m. During moving backscatter collection, any simultaneously deployed zooplankton sampling nets were towed sufficiently astern to avoid echo artefacts. Echosounder receiver noise levels were measured by recording 300 ping data sequences with the transmit pulse deactivated. The resultant noise recordings were used for signal level corrections during subsequent analysis. On autonomous surveys, noise level recordings were conducted either with the ship docked at BIO or operating locally in Bedford Basin. On operator-assisted surveys, noise recordings were typically

[2] As explained in the Preface, the entire DataSonics sounder multiple frequency database been converted to HAC format (Simard et al. 1997; McQuinn 2005). The HAC-converted data includes interpolated times and navigation where those quantities were not directly logged during the original data acquisitions. Computed results in this report were derived directly from the original database using custom in-house analytical software - not from the subsequent HAC-converted data.

repeated several times while at sea at representative acquisition vessel speeds and transducer temperatures.

2.2.3. Analytical Techniques

During backscatter analysis, vertical beam echosounder data were subjected to successive stages of data selection and quantitative processing:

1) Quality Screening – Survey echograms were visually inspected; data were rejected for obvious malfunctions such as sounder TVG failures, excessive interference from other sounders or from vessel electronics, or extended periods of deep signal reduction/dropout resulting from highly aerated water forced under the transducers.

2) Data Selection and Ancillary Parameterization – A subset of the quality-screened data above were selected for subsequent detailed analysis using criteria dependent on the analysis planned. For the mapping of biological distributions using shelf-wide transects virtually all data passing initial quality screening qualified for further processing. Narrower scientific objectives, as in the present report, often required additional selection by locale, water depth, time of day etc. If near-surface features were to be included in analyses, the penetration depths of bubble plumes extending from the surface in rough weather (Zedel and Farmer 1991; Thorpe 1992; Novarini et al. 1998) were tabulated to establish the shallowest permissible depth limit for subsequent echo integration. For the Emerald Basin 200 kHz data used to construct the euphausiid backscatter time series of this report, accepted data were limited to daylight hours. By day, euphausiids commonly aggregate in vertically well-bounded layers in the 220 – 250 m depth range sometimes with isolated dense aggregations or swarms extending upwards to depths of 150 m or so (Cochrane and Sameoto 1987; Cochrane et al. 1991). Usually, the deep euphausiid layers are underlain by horizontally continuous fish layers, principally silver hake (*Merluccius bilineais*). At night, both euphausiids and fish redistribute markedly in depth. The resultant high near-surface euphausiid concentrations were difficult to sample accurately using acoustics due to (sometimes) the transducer draft and, especially, echosounder dynamic range limitations associated with the older technologies employed. Enhanced mixing of euphausiids with fish, fish larvae, and other contrasting near-surface zooplankton populations would be expected to inject further potential uncertainty in nighttime euphausiid estimates. Consequently, nighttime data were not selected for quantitative analysis. In the current report, selected data are limited geographically to the deep central portions of Emerald Basin (usually > 250 m) where dense daytime euphausiid layers are observed well above bottom. Multi-channel echogram overlays (Cochrane et al. 1991) provided observation-based vertical and temporal echo integration bounds to quantify the daylight distributions. The 200 kHz channel (also the 122 and 50 kHz channels in earlier studies) contained both macrozooplankton and fish echoes. The 12 kHz channel, for the most part, revealed fish echoes only and was of the greatest assistance in assigning integration depth bounds to the 200 kHz data so as to minimize unwanted fish echo contamination.

The output of the "Data Selection" phase consisted of a tabulation of acceptable data series for quantitative analysis, defined by file name, start and end file ping numbers, and vertical

integration depth bounds. Associated also with each data series were the necessary ancillary data to quantify the echo integration. These included sounder operational parameters such as transmit level, gain settings, pulse lengths, and bandwidths etc., together with the reference CTD profile for acoustic absorption corrections, the estimated transducer temperature for (transducer) sensitivity thermal correction, and the comparison receiver noise sample. At this stage the basic echosounder combined transmit-receive sensitivity (from tank calibrations), the transducer integrated beam pattern parameter (Clay and Medwin 1977), the transmit waveform envelope (from lab measurements), and the calculated total receiver gain were combined via offline custom software to provide a dataset-specific total system acoustic calibration factor. The calibration factor would be used for full backscatter quantification in standardized acoustic units in a later analysis stage.

3) 1st Order TVG Correction – The sounder-applied time variable gain(s) at collection time (20 log Range + Absorption), present in the relevant sounder input data files, was numerically extended from the sounder TVG expiration range (200 m at 200 kHz) to the maximum profiled depth using the **same fixed** TVG rates as applied prior to TVG expiration. The relevant acoustic database files were read, adjusted accordingly, and rewritten. The earlier Data Selection might be reviewed after this step.

4) Backscatter Computation with 2nd Order TVG Correction – Fully-corrected and properly scaled volume backscattering strength levels were computed from the **squared** 1st order TVG corrected echosounder voltage time series amplitudes on a time-sample by time-sample basis. This process incorporated the above derived system calibration factor, with an additional fine correction for **real** ocean acoustic absorption based upon a parameterized temperature-salinity stratified model, typically 5 – 10 layers for the deep Shelf Basins with absorptions for each layer computed by the theory of Francois and Garrison (1982a, b). Columnar backscattering (water column backscatter /unit area), when required, was obtained by vertical integration over depth of the computed volume backscattering strength expressed in linear (i.e. non-decibel) form. For long transect analysis (not in this report) over which water depths varied significantly, echo integration was performed starting at an assigned beginning depth, for instance 20 meters, and ending either at a second assigned maximum depth, for instance 300 m, or several meters off bottom whichever condition occurred first on a ping-by-ping basis. Usually the column backscatter was averaged over a pre-assigned number of consecutive echosounder pings to produce a tabulated series of along-transect estimates. If either the vessel GPS or vessel log speed fell below 2 knots the relevant data were automatically skipped to eliminate possible quantitative biases arising from station-keeping propeller wakes, reflections from on-station oceanographic instrumentation, or from biological spatial/orientational adjustments induced by the acoustic or light signature of the stationary or near-stationary survey vessel (Sameoto et al. 1985)[3].

[3] Sameoto et al. (1985) demonstrated that exposure of euphausiids to artificial light in the field environment resulted in a near-instantaneous alteration in their associated acoustic backscattering level, the alteration probably mediated by changes in organism physical orientation. During nighttime this rapid light response mechanism could systematically alter observed near-surface euphausiid layer backscatter even for survey vessels travelling at speed. Consequently, it is highly recommended that investigators minimize vessel

For the computation of column backscatter, a further noise correction was applied. This consisted of the linear-form subtraction of a similarly-processed depth-integrated receiver noise sample (section 2.2.2. above) from the previously depth-integrated sounder (biological signal + noise signal) levels - a form of receiver noise cancellation which was frequently of critical importance when processing acoustic data near maximum effective sounding ranges such as in the deeper areas of Emerald Basin.

For the Emerald Basin data of this report, column volume backscatter for a given sampling transect was obtained from ping-by-ping vertical integrations of instantaneous volume backscattering strength between preassigned transect-specific vertical depth bounds sufficient to encompass the euphausiid scattering layers of interest while excluding vertical regions or layers containing fish. The successive ping vertical integrations were averaged in linear form over the span of ping numbers defining the horizontal spatial extent of the chosen transect followed by sounder noise level corrections to yield the transect-averaged column integrated euphausiid backscatter s_a. Next, all individual transect s_a levels computed for central Emerald Basin for a specific sampling survey were themselves arithmetically averaged in linear form employing equal weighting for each transect. This process yielded a single value, survey-specific average column backscatter level together with its attendant statistical error derived from the backscatter variance for the complete set of survey transects. It became standard practice to define two additional column backscatter averages: One average was computed from the subset of survey transects steamed at low vessel speed ($\leq$ 5 knots) while the other average was computed from the remaining set of transects steamed at higher-speeds (> 5 knots). The characteristic low and high vessel speeds were originally associated with the concurrent towing of respective BIONESS or BATFISH sampling platforms (Cochrane et al. 2000). The naming convention was subsequently retained as indicative of vessel speed during data acquisition regardless of whether the named samplers were actually employed.

2.3. ACOUSTIC DOPPLER CURRENT PROFILER (ADCP)

2.3.1. Instrumentation

The ADCP instrument employed for quantitative acoustic backscatter collection was an RD Instruments VM150 operating at 153.4 kHz. This device used four acoustic beams, each oriented downwards at 30º from the vertical, emitted from a hull transducer at either 4.8 or 6.0 m depth from the surface dependent on the vessel platform.

2.3.2. Backscatter Quantification

While typically narrow (~4º) ADCP beams are advantageous in obtaining long range backscatter signals at favourable signal-to-noise ratios, the inclined beam geometry

---

external lighting during nighttime euphausiid surveys. Light-related spatial readjustments for both euphausiids and some fish also occur but these are of a slower nature and consequently of major importance only when the survey vessel is stationary.

imposes an important constraint: Backscatter signals received from the lower 13% of the water column are unusable due to the simultaneous arrival of transducer side-lobe energy reflected off the bottom. Vertical profiles of decibel acoustic backscattering strength, S_v (Clay and Medwin 1977) as a function of slant beam range R, were extracted post-survey using the manufacturer's specified formulae (RD Instruments 1990). The methodology, summarized in Eq. (1) and Table 2, was applied to recorded raw echo intensity counts, E, logged for each individual beam. Echo intensity counts are proportional to the log of the combined acoustic signal and transducer and receiver front end thermal noise contributions without signal spreading or acoustic absorption corrections. During data acquisition, the echo intensity counts were periodically recorded for a sequence of equi-spaced **vertical** sampling bins as described in the VM-ADCP Technical Manual Sept 1991 (RD Instruments 1991).

$$S_v = 10 \log_{10}\left[\frac{4.47 \times 10^{-20} K_2 K_S \left(T_x + 273\right)\left(10^{K_c (E - E_R)/10} - 1\right) R^2}{c \bullet \textit{Pulse Length} \bullet K_1 \, 10^{-2\alpha R/10}}\right] \quad (1)$$

The parameters in Eq. (1) and in Table 2 may be categorized into four groups:

1) Real time continuously monitored variables including raw echo intensity counts, E, transducer temperature, $T_{X,}$ and transmit voltage, V_s

2) Environmental variables, especially the local sound speed, c, and the acoustic absorption coefficient, α, both properties of the water column. The operational temperature of the electronics (receive preamps in transducer head), T_E, may also be considered an environmental variable.

3) Operator-specified or pre-set instrument operating parameters such as profiling emitted pulse lengths and processed vertical bin widths.

4) Instrument-specific calibration parameters either those supplied by the manufacturer, such as the "K" constants, or measured by the user under specified conditions, such as E_{RC} used to compute E_R in Eq. 1.

For quantitative analysis and display, echo intensity counts were reduced to profiles of volume backscattering strength (S_v) versus water-column (vertical) depth. For rigorous application this procedure requires the input of instrument-specific calibrations supplied by the manufacturer, background reference levels established by post-survey tank tests, and internal voltages and temperatures recorded continuously during deployment. Sound speeds and absorption coefficients in Eq. 1 were calculated from CTD profile data collected in three contrasting areas (HL3, LL4, and BBL5) using the methods of Mackenzie (1981) for sound speed, and Francois and Garrison (1982a,b) for acoustic absorption. For the sought accuracies of about ± 1dB, it was sufficient to compute single representative values

of α and c for each area for each survey. S_v profiles were computed for each of the four beams then reduced to geographic point values of S_v by averaging both over depth and along transect as detailed below.

2.3.3. Data Processing

To produce along-track values of average S_v the ADCP ASCII (raw echo count) survey files produced by the RD Instruments Transect program were edited to exclude data records recorded when the ship was on-station (travelling < 2 knots) as also the case for the vertical beam echosounder data. Any data containing high level spikes unlikely to originate from zooplankton backscatter were also removed. Relevant survey tracks were then plotted to delineate the area of the Scotian Shelf covered by each portion of the dataset.
For selected vessel tracks, along-track averages of S_v over depth were computed using one of several data selection (estimate clustering) options: a) Over a specified no. of consecutive ADCP pings b) Over a position group - using all estimates along track until either the latitude or longitude coordinate the current estimate changed by a minimum increment (for instance, 0.5º) from the initial estimate position c) Over a pre-defined distance travelled. To calculate the average echo intensity one first averaged over the intensities recorded on each of the four ADCP beams for each depth layer. The averaging methodology employed was to convert each beam bin S_v in dB into the corresponding linear measure, often denoted s_v in the literature ($S_v = 10 \log s_v$), to enable subsequent arithmetic averaging in linear form, followed by reconversion to decibel S_v as required. Averaging was applied over the four beams, then over the equi-spaced vertical bins (excluding bins affected by bottom echoes), and finally over all pings in each "position group" i.e. an along-track spatial average achieved by averaging over the relevant number of consecutive ADCP transmissions or pings. The overall averaging procedure can be expressed as:

$$\bar{S}_v = 10\log_{10}\frac{1}{4*Nping}\sum_{iping=1}^{Nping}\frac{1}{Nlayer}\sum_{ilayer=1}^{Nlayer}\sum_{ibeam=1}^{4}10^{Sv[iping,ilayer,ibeam]/10} \qquad (2)$$

The average column integrated backscatter, S_a, the quantity plotted and interpreted in this present study, was derived by utilizing the same relation above but multiplying the central summation by the relevant profiled water depth during the overall averaging process. If water depths do not vary greatly within a position group, S_a can be closely approximated by summing the average water column S_v (in decibels) and the log of the average profiled water column depth within the position group. Like volume backscattering strength, S_a is expressed in decibel form. The corresponding linear form, s_a, is related by: $S_a = 10 \log s_a$.

Initially, an attempt was made to carefully calibrate the ADCP systems using the above protocols and to maintain clean, non-contaminated transducer surfaces. Unfortunately, continuity was soon lost in this process. The existence of several differing ADCP systems and transducers whose parts were interchangeable, together with marine fouling of the transducer system which for CCGS HUDSON could only be cleaned by divers or exchanged by dry docking led to subsequent major uncertainties in the instantaneous absolute backscatter calibrations. At minimum, the spatial patterns of zooplankton

backscattering observed within individual surveys should retain validity. In contrast, quantitative comparisons of backscatter levels between surveys should be treated with extreme caution because of known or unknown changes in physical equipment between surveys and probable slow changes in the operational characteristics of the ADCPs over inter-survey time scales. These effects have neither been measured nor quantitatively compensated. With these limitations we nevertheless believe it useful to examine the variation of ADCP backscatter over time (i.e. between surveys) where some valid patterns in biological backscattering may still be discerned – especially considering that fully analysed data regarding Scotian Shelf macrozooplankton abundances and distributions outside Emerald Basin is quite limited.

2.4. BACKSCATTER ACOUSTIC MODELLING

On assuming an ensonified population of **identical** biological scatterers present at a concentration of N /m^3, each scatterer characterized by (identical) acoustic target strength TS measured in the direction of ensonification, the resultant volume backscattering strength S_v is given by[4]:

$$S_v = TS_{dB} + 10 \log_{10} N \qquad (3)$$

Conversely, knowledge of both S_v and TS enables calculation of N. In reality, for even the simple case of a mono-species population, TS for individual scatterers will differ due to variations in physical size and, in the case of elongate macrozooplankton like euphausiids, the scatterer's orientation to the ensonifying beam. If consideration is limited to orientation alone, it is still possible to utilize the form of Eq. (3) provided TS is redefined to be an "effective" target strength, TS_{eff}, obtained by the appropriate statistical average of individual discrete TSs expressed in linear form (i.e. the non-decibel acoustic backscattering cross section σ_{bs}) computed over a representative ensemble of orientations. On assuming scatterers of identical size and of identical internal acoustic properties which differ in acoustic cross section only because of their orientation to the ensonifying beam, then

$$TS_{eff} = 10 \log_{10} \overline{\sigma}_{bs} \qquad (4)$$

Computational techniques for modelling effective target strengths for the case of a vertical beam echosounder were described by Sameoto et al. (1993) and further extended to inclined beam ADCPs by Cochrane et al. (1994). Our approach has been to model euphausiids as straight, finite length, uniform fluid cylinders with major or principal axes orientations described by a probability density function (PDF) of known form. In the field environment, realistic PDFs are most readily obtained photographically in a 2-dimensional form for the sub-population of animals selected so that their major axes orientations lie close to a vertically oriented camera focal plane. The azimuthal distribution of major axes orientations is assumed random thereby precluding the choice of a preferred vertical plane.

[4] These basic acoustic quantities and relationships can be referenced in most ocean acoustics texts such as Clay and Medwin (1977).

The resultant orientational PDF, $P_{2D}(\theta)$, is the probability of the (cylindrical) organism major axis being inclined at angle θ to the horizontal for the above selected sub-population. While published experimental results show considerable variability, we assume a Gaussian form as a starting point:

$$P_{2\text{-}D}(\theta) = \frac{1}{\sigma (2\pi)^{1/2}} \; e^{-\theta^2 / 2\sigma^2} \qquad (5)$$

If the inclinations have a mean tilt, θ_m, to the horizontal, Eq. (5) can be generalized to

$$P_{2\text{-}D}(\theta) = \frac{1}{\sigma (2\pi)^{1/2}} \; e^{-(\theta - \theta_m)^2 / 2\sigma^2} \qquad (6)$$

where, in both cases, σ, the standard deviation of the distribution (not to be confused with the totally different quantity σ_{bs} above) is calculated about the mean orientation.

When averaging spatial orientations in 3-D space, it is conceptually simpler to work with the 3-D volumetric PDF rather than with the 2-D planar PDF function. The 3-D PDF is the probability of an organism drawn at random from 3-D space possessing a major axis orientation lying within a given angular range of the horizontal plane. The 2 and 3-D functions can be related provided the 2-D function does not exhibit a preferred vertical plane (i.e. organism azimuthal orientations are totally random):

$$P_{3\text{-}D}(\theta) \propto P_{2\text{-}D}(\theta) . \cos\theta \qquad (7)$$

In reality, both PDF functional forms tend to fall-off rapidly for large θ. Measured orientational PDFs commonly display sufficient scatter and irregularity that, in practice, there are few observational grounds for not letting the functional form of Eq. (6) to represent initially either the 2-D or 3-D forms of $P(\theta)$ - although once the form of $P(\theta)$ is defined the inter-dimensional relationship of Eq. (7) should be followed for consistency. We will also subsequently demonstrate little computation difference between target strengths derived using either 2 or 3-D PDF forms for given realistic ranges of angular standard deviations. Therefore, one is probably justified in simply defining a 3-D PDF of the form:

$$P_{3\text{-}D}(\theta) = \frac{1}{\sigma (2\pi)^{1/2}} \; e^{-(\theta - \theta_m)^2 / 2\sigma^2} \qquad (8)$$

The latter approach with θ_m and σ defined in 3-D space was followed in Cochrane et al. (2000).

If one assumes a vertical beam transducer of very narrow beamwidth so that the angle of ensonification does not vary significantly over the beam footprint:

$$\overline{\sigma}_{bs} = \frac{\int_0^{\pi/2} \sigma_{bs}(\theta) \cdot P_{3\text{-}D}(\theta) \cdot d\theta}{\int_0^{\pi/2} P_{3\text{-}D}(\theta) \cdot d\theta} \tag{9}$$

Alternatively, using Eq. (7):

$$\overline{\sigma}_{bs} = \frac{\int_0^{\pi/2} \sigma_{bs}(\theta) \cdot P_{2\text{-}D}(\theta) \cdot \cos\theta \, d\theta}{\int_0^{\pi/2} P_{2\text{-}D}(\theta) \cdot \cos\theta \, d\theta} \tag{10}$$

For circular beam transducers of wide beamwidth a more complex formulation is required (Sameoto et al. 1993) where again the 3-D PDF can be substituted, if desired, by dropping the cos(θ) term:

$$\overline{\sigma}_{bs} = \frac{\int_0^{\pi/2} D^4(\gamma) \sin(\gamma) \int_0^{\pi} \int_{-\pi/2}^{\pi/2} \sigma_{bs}(\beta) \cdot P_{2\text{-}D}(\theta) \cdot \cos\theta \, d\theta \, d\phi \, d\gamma}{\int_0^{\pi/2} D^4(\gamma) \sin(\gamma) \int_0^{\pi} \int_{-\pi/2}^{\pi/2} P_{2\text{-}D}(\theta) \cdot \cos\theta \, d\theta \, d\phi \, d\gamma} \tag{11}$$

$D(\gamma)$ is the transducer directivity function (Clay and Medwin 1977) and β the dip angle of the cylinder axis to the plane normal to the line of sight from transducer to target. The azimuthal orientation angle ϕ is measured in the horizontal plane and is defined as the angle between the major organism axis projected onto the horizontal plane and the $\phi = 0^o$ origin, the latter defined by the line joining the scatterer and transducer centers projected onto the horizontal plane. Defining ϕ in this manner introduces a symmetry about the ϕ plane origin that allows restriction of the integration range in ϕ to from 0 to π while simultaneously allowing the scatterer angular distribution function to be defined over a range in θ of either 0 to $\pi/2$ or from $-\pi/2$ to $\pi/2$. The latter range is useful for cases of scatterer asymmetry about the horizontal (i.e. head and tail are distinguished), depending on the reported form of observational measurement. Similarly, the angular distribution functions in Eq. (9) and (10) can also be expanded to the range $-\pi/2$ to $\pi/2$ if advantageous.

$$\sin\beta = \sin\gamma\cos\phi\cos\theta + \cos\gamma\sin\theta \tag{12}$$

The high frequency acoustic transducers used in zooplankton backscatter studies typically have sufficiently narrow beamwidths (< 10^o -3 dB to –3 dB) compared to the range of zooplankton aspect angles that Eq. (10) constitutes a good approximation to the average acoustic backscattering cross section.

For typical ADCPs, acoustic beamwidths are sufficiently narrow (~4º) that the transducer directivity function can be ignored but the large (20 – 30º) ADCP beam inclinations from the vertical must be incorporated in the formulation. The average backscattering cross section of otherwise identical cylinders over an ensemble of orientations, dip angles probability weighted and azimuthal orientations considered random, is given by

$$\overline{\sigma}_{bs} = \frac{\int_{0}^{\pi}\int_{-\pi/2}^{\pi/2} \sigma_{bs}(\beta) \cdot P_{2\text{-}D}(\theta) \cdot \cos\theta \, d\theta \, d\phi}{\int_{0}^{\pi}\int_{-\pi/2}^{\pi/2} P_{2\text{-}D}(\theta) \cdot \cos\theta \, d\theta \, d\phi} \tag{13}$$

where

$$\cos\beta = \sin\xi\cos\phi + \cos\xi\sin\theta \tag{14}$$

The quantity ξ is the transducer beam inclination from the vertical, θ is the 2-D (planar) dip angle of the cylinder to the horizontal, ϕ is the azimuthal orientation of the cylinder axis as measured from the vertical plane coincident with the beam axis, and β, the orientation angle between the cylinder and the plane normal to the acoustic axis of the transducer, or equivalently, the acoustic beam incidence angle onto the cylinder.[5] Again, the range of integration in θ can be restricted to 0 to $\pi/2$ if head and tail are not distinguished – as is the case for the scattering model which immediately follows.

Acoustic cross sections of elongate organisms embedded in seawater are computed from the finite straight cylinder ray model of Stanton et al. (1993) which incorporates an approximation of acoustic modal resonances using geometric ray theory. Relevant formulae appear below:

$$\sigma_{bs} = \frac{L^2}{4\pi} k_1 a \cos\beta \, R_{12}^2 s^2 \left(1 + (T_{12}T_{21})^2 - 2\,T_{12}T_{21}\cos\gamma\right) \tag{15}$$

where

$$s = \sin(k_1 L \sin\beta)/(k_1 L \sin\beta) \tag{16}$$

$$\gamma = 4\,k_2\,a\cos\beta - \frac{\pi}{2}\frac{k_1 a}{(k_1 a + 0.4)} \tag{17}$$

[5] In Cochrane et al. (1994), β was defined as the acoustic grazing angle or the complement of β as defined above. The definition of β has been altered to be consistent with that previously used in our discussion of vertical beam echosounders (above) and as also used in Sameoto et al. (1993).

$$R_{12} = \frac{gh - 1}{gh + 1} \tag{18}$$

and

$$T_{12}T_{21} = \frac{4(gh)^2}{(gh+1)^2} \tag{19}$$

Quantities L and a are the cylinder length and cylinder radius respectively. β is the incidence angle of the ensonifying acoustic wave to the cylinder axis. k_1 and k_2 are the contrasting acoustic wave numbers in seawater and internal to the cylinder respectively, given by $2\pi/\lambda$ where λ is the applicable acoustic wavelength in each medium. s is the directivity function of a fluid cylinder, R_{12} the plane wave reflection coefficient from seawater to cylinder, while T_{12} and T_{21} are the plane wave transmission coefficients, from seawater to cylinder and vice versa. Quantities g and h represent the density ratio and the acoustic sound speed ratio respectively of the fluid cylinder to that of seawater.

Considering a specific euphausiid, L is set equal to the physical body (carapace) length excluding the antennae. The cylinder radius, a, is chosen to match the cylinder and actual euphausiid body volumes. This is achieved by first using a regression relation between equivalent spherical volume radius to euphausiid length borrowed from Greenlaw and Johnson (1982), and then equating equivalent spherical and cylindrical body volumes, thereby allowing solution for a. In M.K.S. units one obtains:

$$a = 0.0289L^{0.79} \tag{20}$$

Computing an average backscattering cross section from Eq. (10), (11), or (13) and possessing a field-measured S_v, the euphausiid number density can be estimated using Eq. (3) and (4). Vertical beam echosounder target strengths at 200 kHz computed for a 2.8 cm *M. norvegica* with physical parameters g = 1.05 and h = 1.03 (Køgeler et al. 1987) for several differing average tilt angles from the horizontal and also for several differing tilt angle standard deviations (SDs) in 3-D space are listed in Table 3. Corresponding euphausiid target strengths at 153.4 kHz for an ADCP profiler beam inclined 30º to the vertical are shown in Table 4.

For the case of the vertical beam sounder and no statistical scatter (i.e. 0º SD) in organism orientation (Table 3) it is observed that effective target strengths (TSs) decline rapidly for non-zero angles of incidence (i.e. organism tilt angles to the horizontal). Consequently, the effective target strength of an elongate organism with a finite statistical distribution of tilts will be critically dependent on the frequency of occurrence of near-zero degree incidence (i.e. essentially broadside) ensonifications. For the vertical beam sounder, effective target strengths drop rapidly when the average organism tilt exceeds the SD of the tilt distribution resulting in comparatively few broadside target ensonifications. For the ADCP which ensonifies using sloping beams the effect is quite complex (Table 4): Maximum target strengths occur for average organism tilts of about 30º – but only if the SD of the tilt angle distribution is very small.

Cochrane et al. (2000) assumed an average *M. norvegica* body inclination of 20º to the horizontal, Gaussian distributed with a SD of 30º based on tenuous observational data, mainly that of Sameoto (1980) and Kristensen and Dalen (1986) which were not in good agreement. The recent northern krill stereo photogrammetry work of Kubilius et al. (2015) supports *M. norvegica* average inclinations of 9 – 17º and SDs of 30 - 37º. For interpretation of the 200 kHz vertical beam sounder data our main interest is confined to daylight hours when euphausiids tend not to be vertically migrating, a process which could affect orientation. Bold typed values in Tables 3 and 4 show computed TSs for orientation parameters bracketing the assumed most probable values. Blue italicized values show the effect of assuming the identical numerical orientation statistics but defined in a 2-D rather than a 3-D space. Clearly, an uncertainty of at least ±1 dB in TS should be ascribed to variable orientation effects. Our assumed orientation parameters (20º Av. tilt, 30º SD) appear to yield average target strengths within 1 dB of those computed bracketing the orientations reported by Kubilius et al. (2015). Orientation effects on euphausiid effective TS may appear less extreme for the single inclined ADCP beam (Table 4) than for the vertical sounder beam (Table 3). In some instances these computed results might be deceptive: Use of a single inclined ADCP beam would make measurements susceptible to non-random azimuthal orientations which might arise from large spatial scale schooling and swarm migration. However, real ADCPs commonly utilize four beams at different azimuths whose backscatter average would tend to minimize any existing azimuthal dependencies. The vertical beam geometry should be virtually immune to azimuthal effects. Observe that use of a working value 20º average euphausiid tilt with a 30º SD results in effective target strengths for both the vertical beam sounder and for the ADCP differing by less than 1 dB from those computed assuming totally random organism orientations. This strongly suggests that the choice of orientation parameters may not be overly critical in many practical modelling applications.

The greatest uncertainty in modelling euphausiid target strengths probably lies with the choice of organism physical acoustic parameters. Cochrane et al. (2000) pointed out that choice of g = 1.0357 and h = 1.0279, as used by Foote (1990) for *Euphausia superba*, rather than our normally assumed g = 1.05 and h = 1.03, would reduce the above modelled target strengths by 2.05 dB. The reader's attention is again drawn to the recent and extensive considerations of krill photogrammetry and resultant target strength modelling of Kubilius et al. (2015). Comparing their 200 kHz SDWBA[6] modelled average TS for 25mm length krill (the first 3 entries in *their* Table 4 which would appear the most relevant to our situation in terms of average organism tilts and SDs) with the results of our above computational algorithm using similar krill body lengths and the same average tilt orientations and tilt SDs defined in a 3-D geometry, and using the Foote physical parameters for Antarctic krill (as quoted above), our modelled TS values appear to be only 1.2 dB higher in each case than those modelled by Kubilius. For a zooplankton species we believe this to constitute a quite reasonable agreement which generally supports the relevance of our modelling algorithms even though the latter are less sophisticated than the modern SDWBA based models.

[6] The **S**tochastic **D**istorted **W**ave **B**orn **A**pproximation model utilized by Kubilius et al. was based on the model of Demer and Conti (2003) improved by Calise and Skaret (2011).

2.5. BIOLOGICAL NET SAMPLING

Zooplankton (including euphausiid) samples were collected using three methods:

- The multi-net BIONESS (Sameoto et al. 1980) equipped with 243 µm mesh nets
- Ring nets for bottom-to-surface vertical tows (¾ m diameter with 200 µm mesh).
- The Continuous Plankton Recorder (CPR) using 285 x 315 µm mesh filters – field CPR usage constituted, during its most recent phase, a contractual sampling program conducted by the Sir Alister Hardy Foundation for Ocean Science in Plymouth England, and to whose historical Scotian Shelf database DFO has also been granted access.

BIONESS and ring net samples were collected on oceanographic surveys in both spring and fall (usually April and October respectively) each year between 1983 and 2004 - not withstanding a few missed sampling periods. Ring net sampling efforts increased from 1995 onwards leading up to the Atlantic Zone Monitoring Program (AZMP) initiating in 1998 which formally adopted the sampling station grid of Fig. 1. CTD profiles were taken on each of the AZMP stations. CPR data were gathered independently at more frequent intervals from commercial vessels (below).

While the BIONESS was used on all stations between years 1983 and 1996, post-1996 BIONESS samples were only acquired on selected stations such as Emerald Basin, Roseway Basin, and the Gully. The BIONESS was towed obliquely from the bottom to the surface at a forward speed of 1.5 m/s while a series of stratified depth samples were collected. The more complete methodology used in collecting BIONESS euphausiid samples has been detailed in Sameoto et al. (1993). Significantly, since 1991 a strobe light has been regularly mounted on BIONESS to minimize net avoidance by, at least, the larger size euphausiids. The use of lights on BIONESS during sampling increased daytime euphausiid catches (at depth) by a factor of 10 – 20 and nighttime catches by a factor of 2 – 3 (Sameoto et al. 1993). Recent observations in the Gulf of Maine by Wiebe et al. (2013) using a strobe light equipped MOCNESS sampler strongly confirmed these effects for euphausiids (mostly *M. norvegica*). Their corresponding abundance factors were about 11.0 by day and 4.5 by night. Their use of artificial lighting also better harmonized net and acoustic backscatter inferred euphausiid abundances strongly suggesting more realistic net abundances when using the strobe (by suppression of a net avoidance response).

CPR sampling and transect locations were detailed in (Sameoto 2001). Briefly, CPR euphausiid samples were collected on continuous along Scotian Shelf transects starting in 1961 and lasting until 1974; sampling was restarted in 1991 and continued beyond 2004, the last reported data included in this report. CPR transects were nominally repeated once a month, with occasional missing months. Average tow depth was 6.7 m. The small 1.27 x 1.27 cm CPR sampling aperture largely restricted reported euphausiid numbers to larval stages with very few reported organisms > 1 cm length. Importantly, the spatial distributions of Scotian Shelf CPR transects in the 1960s and 70s differed significantly from those in the post-1990 period. The vast majority of earlier period transects lay on the inner shelf north of Emerald and LaHave Basins while a minority of transects crossed the

deeper areas of the two Basins. In the latter sampling period, transects were about equally divided between the inner and outer shelves with few, if any, transects crossing the deeper portions of the Basins.

A vital question is whether the shallow depth CPR sampling results might be biased due to the strong diel vertical migration behaviours known to characterize euphausiids since the sampling transects were steamed at unconstrained times of day. At the time of the original analysis, the question was explored by dividing the samples into day and night data. No systematic differences were detectable, the conclusion being that larval stage euphausiids, unlike mature euphausiids, displayed little or no diel migratory behaviour.

The CPR sampling yields, in effect, volumetric population densities (organisms/unit volume). In contrast, our reported quantitative net sampling and acoustic backscatter measures are direct measures of, or are proportional to, columnar population densities (organisms/unit area). Both volumetric and areal densities can potentially serve as proxies for tracking **relative** population trends over time, especially, if the spatial sampling patterns remain fairly constant.

3. ANALYSIS AND RESULTS

3.1. GENERAL

The patterns of variation in underlying biological populations which one wishes to discern from the contrasting sampling techniques, namely conventional and CPR net sampling as well as echosounder and ADCP acoustic backscatter, are all to a greater or lesser extent temporally under-sampled, hence potentially aliased, by the episodic nature of the sampling (discrete spring and fall surveys or monthly CPR transects). Also, since the normal objective is to evaluate long term population variation over extended areas (e.g. the western vs. eastern Scotian Shelf) the question of adequate spatial sampling arises considering that populations will be spatially variant within any specified area. In addition, each data source will possess characteristic limitations in regard to providing population-representative samples. That is, each sampling technique possess inherent biases associated with how they actually sample the desired underlying population, for instance organism physical size biases, repulsion biases, vertical stratification biases, variable degrees of species selectivity, quantization noise from low sampling volumes or excessively localized sampling (i.e. spatial aliasing), and additive electronic noise biases for the acoustic techniques. Often the sampling problems can be ameliorated by using several techniques in combination. For instance, conventional net sampling is frequently subject to spatial under-sampling and low volume quantization noise (particularly for euphausiids) but it also possesses the offsetting advantages of providing precise species identification and organism sizing which can inform the proper interpretation of, for instance, acoustic backscatter, the latter usually less prone to spatial and volumetric under-sampling.

In the interpretations to follow much weight will be given to both the Emerald Basin 200 kHz acoustic backscatter and the wider shelf CPR data. Both methodologies incorporated

inherently high degrees of spatial averaging in their operation and, for the CPR, the advantage of frequent sample repetition which both minimizes and informs the temporal aliasing question. Much less reliable results probably accompany the ADCP backscatter due to its inconsistent calibration and maintenance protocols, undocumented hardware changes, and virtually no data editing to exclude unwanted biological components. For the ADCP, these constitute serious systematic (i.e. essentially non-random) sources of temporal error over and above those related to temporal aliasing and achieving representative samples. Consequently, few deductions from ADCP multi-survey time series should be considered beyond question. Lacking more reliable alternative data, we have, in some instances, been forced to place more reliance on ADCP derived time series than would be otherwise prudent. Often assessments of data reliability and judgements as to the reality of apparent data trends will be quite subjective. The relatively infrequent use of statistical tools has been dictated both by the present lack of the original digital time series and the complex character of the data itself which often tends not to conform to the simple statistical assumptions required for proper use of these tools. With these caveats we proceed to specific results followed by a broader discussion of their significance and interpretation in section 4. Frequently data will be presented separately for the "eastern" and "western" Scotian Shelves and for Emerald Basin. The dividing line between the eastern and western shelves was defined as 61º west longitude, both regions extending seaward to the 200 m shelf-break isobath but excluding Emerald Basin. Emerald Basin was generally defined by the 200 m isobath about its deepest extent.

3.2. ADCP BACKSCATER

ADCP column backscattering strength (s_a) from ADCP acoustic recordings along ship tracks specific to each 1993 to 2005 period Scotian Shelf survey are charted separately for spring and fall survey periods in Figs. 2 and 3 respectively. While calibrations within individual surveys should remain reasonably consistent, the above cautions should be kept in mind.

Attention is drawn to three visual deductions from Figs. 2 and 3:

- The region west of longitude 61° is characterized by higher s_a levels than the eastern half of the study area, an observation further discussed in sections 3.5. and 4.
- The highest s_a levels during both spring and fall generally occurred in the shelf basins in water depths exceeding 200 m. It is in such deep water environments that the large and generally most abundant shelf euphausiid *Meganyctiphanes norvegica* concentrates.
- Spring survey periods are characterized by generally higher s_a values than fall periods. While much caution is warranted in comparing levels between differing surveys, the preponderance and consistency of evidence strongly attests the veracity of this fact. Spring ADCP levels appear to display greater spatial variability across the shelf than those conducted in the fall. The difference between basin and non-basin s_a values was also greatest in the spring.

Some of these observations will be explored on a more quantitative basis in later sections.

3.3. EUPHAUSIID AND MACROZOOPLANKTON POPULATION CHANGES MEASURED BY THE CPR AND CONVENTIONAL NET SAMPLING

The longest duration Scotian Shelf euphausiid data time series were furnished by the CPR (Figs. 4 and 5). CPR-derived euphausiid abundances for the western Scotian Shelf from 1991 to 2004 are, on whole, a factor of ~3 lower than those sampled from 1961 to 1974 (Fig. 4). Western Scotian Shelf euphausiid ring net sampling abundances from 1979 to 2003 are also plotted (Fig. 4) in compatible logarithmic units. The ring net data are characterized by a high degree of scatter as well as sparse spatial and temporal sampling prior to 1995. Visually, ring net abundances show no evidence of any systematic abundance drop within the time gap separating the two CPR sampling intervals. On the contrary, a smoother factor of ~3 abundance *increase* is computed from 1979 to 1993 but this result should be regarded as quite tentative due to the sparse and highly scattered sampling prior to 1995. Hardly more confident is the machine-indicated abundance dip about 1995 and the following peak in the late 1990s even though the sampled data from the mid 1990's onwards contains fewer major time gaps. Moving to the CPR data, for the 1991 - 2004 period, a broad but shallow dip in the mid-to-late 1990s followed by a suggestive modest early to mid-2000s recovery appears present provided the strong seasonal or near-seasonal abundance swings are smoothed. Nevertheless, any **long term** variability in the (nominally) monthly sampled 1991 - 2004 CPR abundances appears considerably lower than that indicated by the spline fit to the simultaneous ring net data. Western Scotian Shelf ADCP backscatter levels are also plotted in Fig. 4 again using compatible vertical axes units (i.e. decibel S_a assumed proportional to log column organism density). Observe that the strong systematic dip in ADCP backscatter beginning in late 2001 would be barely discernible if present in the ring net data at comparable magnitude (we interpret the ring net smoothers as not indicating an analogous dip). A possible connection between pre fall 1991 ADCP trends and smoothed CPR indices is discussed below.

Moving to the whole Scotian Shelf, the spline smoother fit to the ~25 year ring net time series for *M. norvegica* (Fig. 6) might appear indicative of longer term systematic fluctuations. However, as for the western shelf sub-set, the pre-1995 temporal-spatial sampling is sparse and individual measurements highly scattered. In fact, one could legitimately question whether the whole Scotian Shelf has been adequately temporally/spatially sampled to draw any valid conclusions regarding long term trends. Observe that for some surveys only a couple data points purport to speak for the entire shelf, while for better sampled individual surveys the spread in values is 2 – 3 orders of magnitude. Sampled stations differing survey-to-survey combined with an innately high sampling variances conspire to undermine the validity of using successive survey computed population means to discern long term trends. While a straight line drawn through successive centers of the *M. norvegica* spline oscillations in Fig. 6 would imply about a factor of 5 population decrease between 1979 and 2004, we believe this implies nothing with certitude regarding whole shelf very long term population trends. One of the more suggestive short term features, a 1 – 2 order of magnitude population rise beginning about 1995 with a subsequent peak in 1998, is to a degree reflected in the longer term spline fit overlay.

Continuing our examination of the whole Scotian Shelf, visually smoothed monthly CPR euphausiid abundances between 1991 and 2004 (Fig. 5) would appear in slight decline (factor of ~2) through most of the 1990s, prior to a possible slight rise (factor of ~2, perhaps less) starting in the late 1990's and continuing to the 2004 end of data. Overall, the whole Scotian Shelf CPR abundance trends resemble those inferred for the western shelf subset in Fig. 4. Whole Scotian Shelf survey-averaged BIONESS data (Fig.5) in the more frequently sampled 1995-onwards interval appear of inconclusive overall trend, the same appearing true for the Emerald Basin BIONESS data for the same interval. Note the comparative absence of individual whole Scotian Shelf BIONESS samples for the showing high abundances in the fall of 1995 and the very low abundance reported for Emerald Basin for the same survey. In contrast, are the high BIONESS values in 1998 for the whole Scotian Shelf as well as comparatively high valued samples for Emerald Basin, both displaying 1 – 2 order of magnitude rises from 1995. The similarity of the whole Scotian Shelf BIONESS patterns to those noted for the whole shelf ring net samples of Fig. 6 might argue for the validity for these short duration features. While the CPR data of Fig. 5 could be viewed as also supporting this feature, the relevance of larval euphausiids in regard to short to medium span population events is unclear. The acoustic backscatter, examined later, shows little support for analogous short-term features in adult euphausiid populations.

If Emerald Basin BIONESS *M. norvegica* (> 10 mm length) column **wet biomass** is examined dating back to the early 1980s (Fig. 7) a definite upward shift in levels from the 1980s to the post 1995 period is noted. The liberty has been taken to fit a linear regression line to the log of wet biomass (wet weight in grams m^{-2}), the available data limited to two separated time intervals: 1981 to 1988 and 1996 to 2003. The first sample group dated from before use of the BIONESS strobe light while the second group was collected with strobe usage. Taking years 1985 and 2000 as the respective time centers of the two groups, the corresponding regression ordinates indicate an abundance shift by about a factor of 6 (0.8 logarithmic units). However, this factor is in almost exact agreement with the anticipated increase in BIONESS capture efficiency by use of the strobe (section 2.5.). Consequently, for the Emerald Basin BIONESS wet biomass sampling there appears little substantive evidence for any long term trend in **real in-situ** euphausiid abundances from a time period centered on the mid-1980s to a later time period centered on about year 2000. Neither are there obvious visual long-term trends in wet biomass within either grouping examined separately.

In summary, considering the sparse nature of much of the Scotian Shelf conventional euphausiid net sampling from 1979 to 2004, a definitive conclusion regarding very long term (~25 year time scale) abundance trends is probably unwarranted. Future employment of sophisticated statistical tools which properly account for the sparseness of data and the presence of regular patterns of seasonal variability might allow more definitive conclusions. The same conclusions apply to the Emerald Basin conventional net sampling. For the very long duration CPR times series for the western Scotian Shelf, abundance inferences on time scales approaching 40 years might be anticipated since long continuous monthly transects alleviate many of the spatial-temporal under-sampling questions. However, uncertainties related to the major systematic change in sampling patterns

between the two sampled time intervals impede such inferences. At most, within the 1991 to 2004 sampling period, a broad decadal period (factor of ~2) dip in abundances centered in in the late 1990's does appear present for both the Scotian Shelf and the western shelf subset. The general magnitude of this dip is less than the magnitude of superimposed inter-seasonal to inter-annual (1 – 2 year time scale) variability. Again, use of more advanced statistical tools properly accommodating repetitive patterns of short term variability could be more definitive.

3.4. ADDITIONAL INFERENCES FROM NET SAMPLING

While conventional net-sampled abundances may be less than definitive in regard to very long term euphausiid population trends, the degree of scatter characterizing the net sampling does place valuable constraints on the magnitude of any **real** long term biological fluctuations likely to have escaped detection. The scatter may also furnish some indication of the magnitude of future net sampling efforts required to reliably detect systematic changes exceeding a given minimum magnitude. Of immediate importance is the fact that net samples do provide direct information on the species present (including size) and if filtered water volumes can be accurately estimated, the local absolute numeric organism concentrations (i.e. number/m^3) can be directly calculated. Acoustic backscatter sampling, in contrast, cannot directly resolve either species or absolute concentrations. While bulk acoustic measures such as S_v and S_a may be useful for **relative** abundance comparisons, only in the simplest well controlled circumstances can such measures be safely converted to absolute numeric organism concentrations by use of an "effective" organism target strength (for instance by use of eq. (3) section 2.4.). Net sampling can sometimes provide the necessary information to estimate acoustic target strength as well as place important constraints on allowable acoustic interpretations. The latter utility is demonstrated in the arguments immediately following.

To this point it has been implicitly assumed that ADCP vertically integrated backscatter arises mainly from the *M. norvegica* even though integration depth ranges were not restricted to those demonstratively dominated by this species (as for the 200 kHz backscatter). Can net sampling inform this supposition? BIONESS abundances of one alternative macrozooplankton scatterer, decapod shrimp, measured between 1977 and 2003 showed maximum levels in 1996 and in 2000 to 2001 (Fig. 8). As decapods lie in the same size range as large euphausiids they might be expected to contribute to the backscattering by an amount equal to or only slightly greater than euphausiids **at the same numeric abundance**. However, Scotian Shelf decapod column abundances are 1 – 2 orders of magnitude lower than those of *M. norvegica* (Table 6) which likely make their contribution to column acoustic backscatter insignificant for our purposes. Other macrozooplankton and micronekton were also present in the net samples (Table 6), but apart from the chaetognaths they represented a small percentage of these total two groups.

Large copepods such as *C. finmarchicus* copepodite stages 4 to 6 when present in very high concentrations may, at times, contribute noticeably to the 153 kHz ADCP backscattering. However, this contribution is usually less than that arising from adult *M. norvegica*. For instance, our acoustic scattering models predict an acoustic target strength of about -119 dB

for a 2.5 mm *C. finmarchicus* (assuming g = 1.00 and h = 1.03) at 153.4 kHz (TS ≈ 115 dB for the 200 kHz vertical beam sounder) compared to an effective target strength of about -74 dB for an *M. norvegica* using inclined ADCP beams (an effective TS also ~ -74 dB at 200 kHz for the vertical beam sounder) assuming typical randomness in *M. norvegica* orientations (Tables 3 and 4). Comparison of the two ADCP beam target strengths implies that the column density of *C. finmarchicus* would have to exceed that of *M. norvegica* by 4 to 5 orders of magnitude to generate comparable levels of backscatter. Typical observed **column** abundance ratios for these two species from our ring net sampling (Fig. 6) are about 3 orders of magnitude, and probably even less, since ring nets inefficiently sample larger euphausiids. While the abundances of *C. finmarchicus* collected with *M. norvegica* in the same net samples sometimes showed suggestively similar patterns of change over time as those for *M. norvegica* it appears unlikely that the *C. finmarchicus* populations significantly influenced the patterns of change seen in the ADCP data (and similarly in regard to the vertical beam 200 kHz sounder data).

Another zooplankton genus with the potential to cause significant backscattering at the acoustic frequencies used in this study is *Limacina* spp. These planktonic gastropods or sea-snails due to their hard-shelled nature possess relatively high acoustic target strengths for their size or biomass (Stanton et al. 1996). The yearly abundance of *Limacina* spp. on the shelf is shown in Fig. 6. The multi-year abundance pattern of *Limacina* spp. appears to reflect those of *C. finmarchicus* and, maybe to a degree, *M. norvegica*.[7] However, *Limacina* is believed to be a weak diel vertical migrator on the shelf (this fact could bear further investigation). Our frequent observation of strong diel migration patterns, a known characteristic of euphausiids, in the principal backscattering layers over wide regions of the Shelf, most probably rules out *Limacin*a as a major contributor to the overall ADCP backscattering. In addition, more recent compilations of Atlantic Canada ring net seasonal cumulative abundances for *Limacina* spp. reveal, on average, slightly higher abundances in the fall than in the spring (Catherine Johnson DFO/BIO, unpublished data, contrary to the observed seasonal trends for the ADCP backscatter – and for the 200 kHz Emerald Basin backscatter discussed below. While conventional zooplankton net sampling may rule out several alternative explanations for the dominant origin of ADCP backscatter, the question is not firmly settled. Juvenile pelagic fish over wide areas of the Scotian Shelf and nighttime silver hake in the inner Shelf Basins could still be significant column scatters at select times and locations.

It is frequently assumed, often implicitly, that population trends inferred by applying one sampling methodology to a specific organism constitute unbiased estimators of trends in the **whole population** of the same organism. However, all sampling techniques have inherent biases even for a single class of organism. For instance, it is known that **large mobile** euphausiids and decapod shrimp are sampled more efficiently by the BIONESS (and for at least euphausiids, the strobe-equipped instruments) than by the vertically deployed ring nets. Similarly, the acoustic backscatter measured from euphausiids is

[7] One is likely on a modestly firmer footing in discerning similar patterns of abundance variation between contrasting species measured on the same surveys and often at the same stations as in Fig. 6 than in further implying that these same patterns of abundance also adequately characterize variations in whole shelf populations.

heavily weighted toward the physically larger size fraction present, especially adult *M. norvegica*. CPR euphausiid counts consist almost exclusively of the physically smaller sized (< 1 cm length) larval stages of the population. Might sampling biases also bias inferred trends in the underlying populations? Ideally, one would like to demonstrate that whole populations and biased samples of the same populations move largely in lock-step.

This has practical implications in how we might analyse or interpret survey results. Consider the net sampling for euphausiids. The BIONESS database/time series is smaller and geographically more restricted than the ring net database. The ring net and BIONESS capture euphausiids of < 1 cm length with about equal efficiency. Therefore, if the smaller euphausiids have similar temporal and geographic distribution patterns to the larger euphausiids it should be possible to use the ring net data to supplement the more accurate BIONESS data (i.e. the population trends delineated by the two types of net sampling should be similar and representative of that of the total underlying population). The data of Fig. 9 constitutes an initial attempt to directly explore this issue. Mean column numbers for Scotian Shelf euphausiids < 1 cm length collected with ring nets, and euphausiids > 1 cm length collected with the BIONESS are overlaid and spline fitters applied. It is best left to the reader to judge if the size linkages implied by what we believe to be quite similar oscillation patterns in the spline fitters are truly real. At the very least, this experimental approach might be repeated more definitively with newer data covering both large and small euphausiids sampled at the same stations on each survey.

Clearly, annual biological reproductive and developmental cycles will set limitations in how well sampling biased as to physical size, for instance, actually mirrors a population as a whole. However, it would seem not illogical that some loose relationship should persist between total populations and biased samples of this population, particularly if such population estimates are smoothed over time intervals equal to or exceeding the typical duration of reproductive cycles and provided the choice of sampling times is not overly pathological. (Note that the Fig. 9 data for both large and small euphausiids do appear to support the previously noted population dip in 1995 and later peak in 1998).

3.5. VERTICAL BEAM ECHOSOUNDER BACKSCATTER

For this report, 200 kHz vertical beam echosounder data was limited to Emerald Basin. Further restricting the analysed data to daylight hours ensured euphausiid layers were deep, comparatively concentrated in the vertical dimension, and little contaminated from embedded fish. Within individual surveys, on employing the narrowest possible vertical integration bounds to exclude pelagic fish layers and other unwanted scatterers, average $s_a = \int s_v dz$ was computed for each selected sampling transect (usually short to restrict the sampling to the central Basin). Resultant s_a values for individual transects were subsequently arithmetically averaged using equi-transect weighting to produce a single-valued survey mean tabulation. The complete 27 year, 1984 to 2011, generated time series of survey mean s_a is shown in Fig. 10. The same data plotted separately for spring and fall surveys appears in Figs. 11 and 12 respectively. Statistical errors (SE) associated with individual survey mean s_a values are also shown in the same figures when more than one survey transect was averaged in mean value generation. A 5th order polynomial curve has

been fitted to the data of Fig. 10 to provide one type of more objective assessment of the long term trend in s_a, especially the location of the population maximum. Emerald Basin backscatter analyses performed prior to November 1996 were reported in Cochrane et al. (2000).

Within any single survey, individual transect measures of s_a were highly repeatable as attested by the relatively low S.E.s in Fig. 10 when considered in the light of the typically low degrees of freedom listed in Table 7. Another test of acoustic data consistency was the comparison of separate mean s_a's for "BIONESS" and "BATFISH" type transects steamed at contrasting vessel speeds (Fig. 13). The relatively small differences attest to the absence of marked speed-dependent sampling inconsistencies. Inferred column euphausiid biomass densities (g/m^2) are plotted along the right axis of Fig. 10. The biomass densities were derived using a model-derived effective euphausiid target strength of -74.8 dB (Table 3), as numerically computed for identically sized 2.8 cm length organisms characterized by a 3-D Gaussian tilt distribution of 30º SD about a 20º mean tilt (Table 3). The columnar biomass density is the product of the columnar numeric concentration $\left(s_a / \overline{\sigma_{bs}}\right)$ and the mass of an individual euphausiid, the latter computed from the length-to-volume regression of Greenlaw and Johnson (1982) while assuming a euphausiid density only slightly higher than seawater.

It is instructive to compare the central Emerald Basin vertical beam 200 kHz echosounder s_a levels with the ADCP integrated backscattering levels gathered from the mid-1990s onwards (Fig. 14). Selected Emerald Basin ADCP data were restricted to water depths exceeding 200 m for reasonable compatibility with the vertical beam echosounder measurements.[8] The 200 kHz data representation in Fig. 14 differs from that in Fig. 10 in that (200 kHz) data points have been plotted only for surveys in which ADCP sampling was also conducted. Even apart from the system-specific differences in acoustic frequency and ensonification angle, quite different measures are actually being compared: Vertical beam sounder backscatter levels have been selected for daylight sampling times and for vertical integration depth ranges that best isolate the euphausiid component. In contrast, ADCP backscatter has been vertically integrated from the near-surface to about 87% of the water depth (section 2.3.2.) without regard to time of day and, consequently, contains relatively higher unwanted contributions from silver hake and other pelagics. On integrating ADCP levels in the 200 - 270 m bathymetric depths characterizing central Emerald Basin, the bottom 26 - 35 m is necessarily excluded. During daylight, this exclusion is frequently significant for euphausiids, but also advantageous in eliminating intense unwanted backscatter from near-bottom pelagic fish layers underlying the euphausiid layer(s) at depth.

In spite of ADCP calibration uncertainties and contrasting sampling protocols, column backscatter levels from the two differing acoustic instruments when compared in logarithmic units over multiple whole surveys (Fig. 15) do display a positive and significant linear correlation ($r = 0.75$, standard T-test significant at better than $P = 0.005$ level) with linear regression slope = 0.91 using the assumed more reliable vertical beam log

[8] The actual depth may have been higher, see footnote immediately following.

s_a as the independent variable and excluding the data point for decimal year 1993.38 (not plotted) as an outlier. A unity slope linear regression fit to the decibel form scatter-plot would be expected if both techniques sample the same populations in an identical manner – which is unlikely to be the case for reasons stated previously and the fact that less detailed acoustic absorption corrections were applied to the ADCP. ADCP backscatter level deviations from the linear regression line are typically 3 – 6 dB. The best correlation between ADCP and 200 kHz measures appears to lie in the time interval between fall 1995 and spring 2001 (Fig. 14). The visually lower correlations prevailing from fall 2001 onwards may arise from less accurate ADCP calibrations (section 2.3.3.). However, after the sharp dip in both 200 kHz and ADCP backscatter beginning in the fall of 2001 and persisting onwards for several years, backscatter levels, especially those from the 200 kHz sounder, were very close to the instrumental noise floor where small errors in the applied sounder noise corrections could introduce relatively large deviations in resultant s_a estimates. Also, any backscatter distortions induced in either instrument by inclusion of (unwanted) embedded fish echoes would be enhanced during periods of low euphausiid backscatter. Nevertheless, the reasonably good correlation between Emerald Basin ADCP and 200 kHz backscatter measures (Figs. 14 and 15) would argue that the ADCP measures do possess sufficient validity to permit some cautious interpretation of their time variability, especially for the wider shelf where analysed 200 kHz sounder data do not exist.

3.6. BACKSCATTER ACOUSTIC TRENDS AND CORRELATIONS

We now examine in greater detail how euphausiid acoustic population measures vary over time and compare between differing shelf areas. Also explored is the correlation of acoustic population measures with select environmental variables potentially driving population change. Multivariate correlations between Scotian Shelf CPR "total euphausiids" and several oceanographic and meteorological variables were reported without elaboration in Sameoto (2001) where total euphausiids appeared to correlate positively with the frequency of major storms, and to correlate negatively with the phytoplankton colour index and the average upper 50 m ocean temperature anomaly. Several new correlations are now explored using, in particular, the 200 kHz Emerald Basin backscatter time series.

In regard to observed acoustic backscatter levels the following observations are made:

- In Emerald Basin, 200 kHz euphausiid column backscatter levels display high inter-seasonal and year-to-year variability (Fig. 10). When **highly smoothed,** backscatter levels appear to rise by a factor of 3 or 4 from the mid-1980s to peak in 1994 – 95 then slowly decline by a factor of 2 – 3 to around 2005 with no clear long term trend to the 2011 end of sampling.
- Emerald Basin spring euphausiid backscatter levels are about a factor of 2 higher and more variable year-to-year than corresponding fall levels (Figs. 11 and 12). Both spring and fall levels generally decline from the mid-1990s to at least the mid-2000s, the decline appearing more marked and regular for the fall levels.
- In Emerald Basin, the fall of 2001 ushered in a period of comparatively low 200 kHz (unsmoothed) euphausiid backscatter levels persisting through 2003.

- Emerald Basin ADCP column backscatter levels (Fig. 16) are comparatively high from 1993 to 1995 (a broad peak), decline slightly during the mid-to-late 1990s with indications of a recovery in 2000 and early 2001. Subsequently, unsmoothed levels drop precipitously in the fall of 2001, analogous to the 200 kHz observations, followed a partial recovery in 2003 and 2004.[9]
- Eastern and western Scotian Shelf ADCP unsmoothed column backscatter levels (Fig. 16) rise systematically through the 1990s before marked drops in the fall of 2001 not unlike those observed in Emerald Basin. Generally rising ADCP trends through the late 1990s contrast with the trend in Emerald Basin which remains level or slowly declines prior to the prominent drop in the fall of 2001.
- In spite of modestly contrasting long term trends, ADCP backscatter levels in Emerald Basin are roughly a factor of 2 higher than those on the western Scotian Shelf which, in turn, are about a factor of 2 higher than those observed on the eastern Scotian Shelf.
- Both the contrasting abundance levels and differing abundance trends between Emerald Basin and those of the wider shelf regions are evident from individual year-by-year backscatter comparisons making these conclusions fairly insensitive to (unknown) changes in ADCP calibration over time.
- No obvious *visual* correlations are observed between ADCP backscatter levels for either the western or eastern Scotian Shelf and smoothed bottom temperatures for the western shelf (Fig. 17).

We now consider potential relationships between Emerald Basin deep temperatures and inferred euphausiid populations. Emerald Basin below 150 m depth is nearly isothermal. Deep Basin temperatures fluctuate over time from occasional incursions of warm saline slope water (Petrie and Drinkwater 1993) or flushing events involving colder slope waters with a larger mixed fraction of Labrador Current origin. Years of higher Labrador Current transport result in cooler slope waters (Drinkwater et al. 2003). A plot of deep Emerald Basin temperature[10] vs. time appears in Fig. 18 while a scatter plot of survey-averaged 200 kHz sounder s_a (log scale) vs. deep Emerald Basin temperature (T) over the same interval appears in Fig. 19. Inspection of the deep Emerald Basin temperature time series (Fig. 18) reveals two cold water influxes, each of abrupt initiation and limited duration:

- The first influx occurs between the 1997 fall survey and the 1998 spring survey as independently detailed by Drinkwater et al. (2003).
- The second influx initiates between the spring 2006 and fall 2007 surveys, is of longer duration, and consists perhaps of two back-to-back events.

Ignoring these two cold events, visible similarities are observed between the time dependencies of temperature (Fig. 18) and s_a (Fig. 10), both dependent variables broadly

[9] The alternative ADCP backscatter Emerald Basin time series presented in Fig. 14 is characterized by both higher amplitudes and higher relative variances than the similar denoted entity in Fig. 16. Differing data selection criteria were evidently employed, the specifics being no longer accessible. We conjecture that the data analysed to construct Fig. 14 constituted a sub-set of that utilized for Fig. 16, the former data being restricted to the deep central portions of Emerald Basin, perhaps bottom depths > 250 m, in contrast to 200 m used for the latter. The deeper depths would better correspond with to the 200 kHz echosounder data selection criteria.

[10] Temperatures obtained from our survey-specific measurements.

peaking in the mid-1990s. On performing a linear regression of the Fig. 19 scatter plot data, a slight positive correlation between log s_a (or equivalently S_a, since $S_a = 10 \log s_a$) and T was observed (r = 0.29, p = 0.10). Elimination of the 3 data points with T < 7.5º C associated with the two major cold events, increased r to 0.31 with p dropping to 0.04. We view the positive correlation as strongly suggestive but not conclusive, even though the nominally computed uncertainties are low: Much variation is observed to be of a long term character. Successive estimates of s_a and of T both strongly auto-correlate thereby reducing the effective independent degrees of freedom in the analysis. Consequently, while a modest positive correlation between log s_a and deep Basin temperature exists, a correlation which increases when the low temperature outliers are removed, the true statistical significances are considerably less than those classically computed. Correlations between seasonally separated spring and fall log s_a and deep basin temperature were also weak, although the correlation for the fall data (r = 0.30, no outliers removed) exceeded that for the spring (r = 0.19, no outliers removed).

A quite different alternative possibility is that the residual correlations are artefacts of imprecise backscatter corrections for water column acoustic absorption in a changing thermal environment. Detailed examinations shows this can be discounted as the applied Emerald Basin absorption corrections were computed using locally measured TS profiles and the probable magnitude of remaining absorption errors should be insufficient to produce the observed correlations.[11]

Environmental determinates of Emerald Basin euphausiid column abundances could extend to influences of a widespread character and could involve significant time delays. Such a potential correlate could be the atmospheric North Atlantic Oscillation (NAO) (Petrie 2007). The NAO strongly influences North American east coast weather patterns, especially winter air temperatures. NAO environmental influences could act on a variety of spatial/temporal scales: Associated wind and temperature fields can act locally, controlling shallow water temperatures and stratification by direct interactions with limited delays. On broader spatial/temporal scales, NAO-associated wind fields constitute a forcing function for the peripheral circulations of the North Atlantic Basin including the Labrador Current and its local Scotian Shelf expression, the Nova Scotia Current (Drinkwater 1996). In this case, Scotian Shelf effects might be mediated by less direct and potentially more delayed advective processes. The NAO monthly index (NWS Climate Prediction Center 2014) for the years 1980 - 2012 with superimposed 1 year and 5 year **causal** running means is plotted in Fig. 20. Observe especially the interval of dominantly positive smoothed indices characterizing the early to mid-1990s, these constituting the highest NAO values in the Twentieth Century (Hakkinen and Rhines 2009). The upward NAO trend shown by the 5 year causal running mean and extending back to at least 1980 (Fig. 20) is observed to peak near simultaneously with the smoothed 200 kHz s_a levels in Emerald Basin (Fig. 10). This observation is further treated in the Discussion section below.

[11] The 2-way cumulative absorption difference at 200 kHz between a "cold" (4º C, 34.5 ppm) and "warm" (10º C, 35.1 ppm) deep Emerald Basin between 150 and 260 m depth would be about 2.2 dB. For the 153.4 kHz ADCP the difference would be about 2.4 dB after incorporating the additional correction for slant range – although, in practice, the ADCP cannot actually sample central Emerald Basin backscatter deeper than about 235 m or 87% of the water column depth below the transducer (see section 2.3.2.).

4. DISCUSSION AND CONCLUSIONS

4.1. THE CHARACTER OF SPATIAL – TEMPORAL VARIABILITY

Several characteristics of the acoustic backscatter data deserve further elaboration. First, is the high consistency between multiple Emerald Basin 200 kHz column backscatter estimates generated during the course of any individual survey (i.e. low **intra**-survey variability) reflected in the low S.E.s in Figs. 10 - 12 including the agreement between survey sampling variants in Fig. 13. Second, in contrast, is the high **inter**-survey variability which we interpret as primarily reflective of true survey-to-survey population variability. The low **intra**-survey variability is believed a consequence of both relative stability in the underlying biological population over the duration of a single survey and the reliable estimation of indices of this population due to the high total water volumes non-redundantly ensonified for individual estimates (i.e. high degrees of spatial and volumetric population averaging).

One interpretative limitation in regard to **inter**-survey and longer time scale variability is the unknown degree of temporal aliasing arising from the recurrent pattern of spring and fall survey sampling. This potentially affects not only acoustic but also conventional net sampling. While individual backscatter measures in Emerald Basin usually correlate well over the ~1 week duration of individual surveys, survey-averaged backscatter measures readily decorrelate on the ~ 5 – 6 month inter-survey time scales. Some, but not all, of the inter-survey backscatter fluctuation arises from systematic seasonal biological variations. Euphausiids are expected to (and normally do) display their largest biomass in the spring since the previous year's generation has reached adulthood and are ready to reproduce. *M. norvegica* live up to three years but most individuals die after spawning in the second year. This die-off results in a drop in biomass after spawning which occurs during June and accounts for the much lower biomass and consequent lower s_a values observed in the fall. Other euphausiid species are also present but these are characterized by very patchy distributions and are generally less common than *M. norvegica* (Table 5). The smaller euphausiid *Thysanoessa longicaudata* was slightly more common in total survey samples; however, this species is concentrated along the Scotian Slope and is less common than *M. norvegica* on the shelf itself. The smaller euphausiids probably contribute little to the observed acoustic backscatter.

The CPR euphausiid profiles sampled (nominally) monthly may provide some clues as to the **maximum** severity of such effects. Fluctuations in highly spatially averaged Scotian Shelf CPR larval abundances by a factor of 4 – 10 are observed over time intervals as short as several months in Figs. 4 and 5. The more mature euphausiid developmental stages sensed by the acoustics may well fluctuate less in the short term. However, within LaHave Basin, column backscatter from diel migrating scattering layers, most likely adult *M. norvegica*, continuously monitored for 49 days by a fixed bottom-mounted ADCP (Cochrane et al. 1994) was observed to systematically shift by about a factor of 5 (7 dB) over time scales as short as 10 – 15 days (Cochrane et al. 1994). While these single location observations may not be representative of the total population, it should signify

caution in summarily dismissing temporal aliasing as an important constraint on our survey-based sampling. Nevertheless, in the absence of more definitive information we will proceed assuming that the inferred systematic multi-year to decadal time scale shifts in daytime deep Emerald Basin 200 kHz backscatter levels do reflect long term population trends with reasonable accuracy.

4.2. ACOUSTICS AND NET SAMPLING

Further consideration of the Emerald Basin 200 kHz backscatter may inform previous results and conclusions. We have already seen that the general shift by a factor of ~ 3 – 4 in nominal wet biomass between the two separated intervals of intensive BIONESS sampling (Fig. 7) is fully explicable by the increased sampler efficiency associated with strobe light usage. Similarly, the Emerald Basin 200 kHz time series of Fig. 10 might suggest a factor of ~2 population rise between the same two time intervals. However, a x2 real population shift is probably insufficient for one type of sampling to reliably inform the other considering the degree of BIONESS scatter in Fig. 7 and remaining uncertainties regarding the precise effects of strobe usage. In Fig. 5, an abundance drop by a factor of ~7 is noted for BIONESS-sampled Emerald Basin euphausiids between the 2001 spring and fall surveys, a factor not incompatible with the marked downward shift in 200 kHz backscatter. Nevertheless, other peaks and troughs in the Emerald Basin BIONESS abundances in Fig. 5 are difficult to convincingly correlate with either the 200 kHz acoustics or with the Emerald Basin ADCP backscatter therefore placing the significance of the 2001 BIONESS shift in doubt. The issue is probably more one of insufficient BIONESS sampling to yield highly confident results rather than the BIONESS data necessarily contradicting the acoustics.

The statistical robustness of the BIONESS sampling is even more problematic for the wider shelf regions (Fig. 5). **Within** individual surveys, discrete station euphausiid column densities can range over 3 – 4 orders of magnitude, a typical number of sampling stations being 6 or less. Clearly, we are dealing with populations possessing extreme spatial variability exacerbated by the fact that not all nominal sampling stations are necessarily visited on every survey. Under these circumstances it seems unlikely that any type of data averaging or smoothing can do justice to estimating or tracking wide-area total populations – the populations are irretrievably under-sampled. Ring net column densities within individual surveys (Fig. 6) range through a comparable ~3 orders of magnitude. It would be beneficial to better understand the degree to which the tendency of euphausiids to aggregate at very short spatial scales ("krill swarms" etc.) exacerbates the net sampling problem. Curiously, quite similar degrees of single survey scatter characterize Limacina ssp. and C. finmarchicus (Fig. 6) – so the issue is not fully understood. Our experience with Emerald Basin 200 kHz acoustic imagery is that prevalence of well resolved swarms varies from survey-to-survey. Commonly, the deep daytime euphausiid layer displays a diffuse, virtually featureless appearance, but the ability of a 5º transducer to resolve lateral features smaller than about 30 m at ~270 m depths is limited and the long 5 ms pulse length also produces considerable smoothing in the vertical dimension. Isolated resolved swarms, when visible, tend to lie above the diffuse euphausiid layer.

Some outstanding issues regarding CPR euphausiid sampling have been intimated. One question is whether surficial CPR samples of small and immature euphausiids bear any close quantitative relationship to an underlying more mature euphausiid population. A second question concerns potential biases introduced by the change in sampling patterns between years 1961 – 1974 and 1991 – 2004, the nominally sampled populations being a factor of ~3 higher during the former period than during the latter. The earlier period CPR transects were heavily biased toward the inner Scotian Shelf where the prevailing Nova Scotia Current might be expected to be stronger and more heavily influenced by the Gulf of St. Lawrence outflow. Observe that a *linear* factor of ~3 population change is a relatively small variation compared to the typical spread for single survey ring net data in Fig. 6. What might be concluded from the CPR time series of Figs. 4 and 5 is that any credible multi-year trends are of considerably lower magnitude than the typical longer term trends indicated by fitting smoothers to conventional net-sampled data. While the CPR and conventional nets usually sample quite different euphausiid developmental stages it would seem logical that when **smoothed over multi-year time spans** both entities should fluctuate roughly in harmony with an underlying population. If large discrepancies in trend are observed, one interpretation is that the spatially wide-ranging and frequently sampled CPR data when suitably smoothed over time furnishes a truer index to long term population shifts than conventional nets, the latter prone to spatial and temporal under-sampling frequently resulting in spurious nominal population trends. One critical question is whether the small larval euphausiids sampled by the CPR actually undergo diel migration (we have concluded that they do not), a topic for further investigation.

ADCP euphausiid sampling shares with CPR sampling the inherent advantages of wide-ranging and spatially continuous coverage. ADCP sampling possesses the additional advantage of (typically) many orders of magnitude greater total sampled water volumes compared to CPR sampling. Offsetting ADCP disadvantages (for the present datasets) include uncertain survey-to-survey calibrations, non-selectivity as to scatterer type, and possible temporal aliasing from repetitive spring and fall survey sampling. Within the 1993 – 2004 ADCP measurement period (Fig. 16) the longest discernible backscatter trends (i.e. ignoring fluctuations < 1 – 2 year period) appear to fluctuate by only a factor of 2 – 3 in magnitude. Because of the ADCP's potential to discern modest population trends, well averaged spatially, the ADCP backscatter levels might be expected to be more akin in character to CPR population estimates. Are long term trends visible in the ADCP and CPR datasets in agreement? The best (fewest gaps combined with widest coverage) ADCP dataset in Fig. 16 is probably that from the western Scotian Shelf. The ADCP would indicate a ~50% rise in smoothed backscatter from the mid-1990s into early 2001, in reasonable agreement with the magnitude of the CPR trend over the same interval (Fig. 4). However, the CPR data shows no clear sign of the extended population crash starting in the fall of 2001 very evident in the acoustics (nor is similar crash evident in the whole Scotian Shelf CPR data detailed in Fig. 5). Visual smoothing of the whole shelf CPR data of Fig. 5 would argue for a broad euphausiid population minimum around 1997 with abundances roughly a factor of 2 higher in both the early 1990s and the mid-2000s (comparable to those for the isolated western Shelf). Again, we emphasize these constitute subtle population shifts which would be hardly discernible if present at the same magnitude in conventional net-sampled abundances as plotted in Fig. 6. Interestingly, both the ADCP data (Fig. 16)

and the 200 kHz backscatter acoustics (Fig. 10) argue for somewhat different long-term trends in Emerald Basin from the mid-1990s to fall 2001 as compared to those observed (by the ADCP alone) for the remainder of the shelf, namely level or downwards for Emerald verses upwards for the eastern and western shelves and, by inference, for the whole Scotian Shelf as well.

4.3. LIMITATIONS

Despite noted interpretational consistencies, uncertainties persist, some already elaborated, others raising more fundamental issues:

- The widespread Scotian Shelf (including Emerald Basin) euphausiid population dip by a factor of 4 – 8 delineated by the acoustic backscatter in the 2001 – 2002 period (Figs. 10, 16, and 17) has no clear visual analogue in the CPR data, nor is it unambiguously observed in the highly scattered conventional net data.
- The factors responsible for the markedly contrasting 1990s ADCP backscatter trends between Emerald Basin and the larger western and eastern shelf areas remain unknown.
- The ADCP backscatter time series, serving as indices of euphausiid abundance, may have been over-interpreted considering the lack of proper calibration controls and little effort to exclude non-euphausiid scatterers.
- The compatibility of pre and post 1980 CPR population measures remains uncertain considering the shift in spatial sampling patterns.
- Monthly sampled CPR abundances fluctuate strongly and systematically on 1 – 2 year time scales often with significant variation over time scales of just a few months. These annual or slightly longer period fluctuations are comparable to if not higher in amplitude than the inferred magnitude of decadal scale trends. This raises legitimate questions regarding the sufficiency of the twice yearly acoustic and net survey sampling to accurately define multi-year to decadal euphausiid population trends. Temporal under-sampling effects could be further exacerbated by inconsistent annual survey dates (i.e. sample time jitter), deviant sampling patterns between surveys (i.e. spatial sampling inconsistencies), and occasional missed surveys.
- CPR-sampling of mainly larval euphausiids may not consistently track the long term fluctuation trends in more mature developmental stage underlying populations.
- Conventionally net-sampled euphausiid abundances at multiple stations for individual surveys typically display several orders of magnitude scatter believed due to the sparse and near point sampling of highly spatially variant natural populations. This fact combined with the normally low and varying number of survey sampling stations implies that any long term population trends derived from conventional net sampling are very questionable.
- From an analytical perspective, has sufficient attention been paid to whether population data have been assimilated in linear or logarithmic forms for the purposes of regression line and trend fitting? Trend fitting is a type of data averaging with potentially quite different results depending on how this is achieved. For instance, logarithmic averaging tends to deemphasize local population “hotspots” and does not implicitly conserve backscattered energy or proportionate total populations. In

contrast, acoustic backscatter has traditionally been averaged in linear (i.e. s_a) form. Risking oversimplification, fisheries acoustics usually attempts estimation of a total stock which over short time spans is conserved in spite of the spatial distribution it might instantaneously assume. Comparison of population trends derived using linear measures with trends derived using logarithmic measures could be misleading.

4.4. MULTI-TROPHIC LEVEL VARIABILITY

The apparent CPR-delineated declines in (larval) euphausiid populations during the early to mid-1990s on both the western and the entire Scotian Shelf do resemble measured zooplankton population trends one trophic level lower: Sameoto (2001) reported Scotian Shelf CPR trends for the dominant copepod *Calanus finmarchicus* populations (stages 1 – 4 and 5 – 6). Sameoto's Fig. 3 showed copepod abundances declining almost continuously from 1991 to the 1998 study termination. A downward abundance trend is also evident in the spline-fitted *C. finmarchicus* data displayed in (this current report) Fig. 6 where a broad dip appears centered about 1996-97.[12] The latter Calanus dip is virtually coincident with the broad dips in CPR-delineated euphausiid populations in Figs. 4 and 5 but no analogous dip is clearly discerned in the euphausiid ring net sampling data (also Fig. 6) or in the ADCP data (Figs. 16 and 17). The environmental correlates associated with lower trophic level populations could easily extend to higher trophic level populations. For instance, Sameoto (2001) noted that both Scotian Shelf CPR-observed *C. finmarchicus* stages 1 – 4 and total euphausiids display a significant negative correlation with the average upper 50 m water temperature anomaly. Our present data (section 3.6.) suggested a modest positive correlation between acoustically delineated (200 kHz) Emerald Basin euphausiid abundances and **deep** Basin temperatures, Emerald Basin upper 50 m temperature anomalies appearing little correlated with those at depth based on temperature data from the mid 1980's to the mid-1990s examined by Drinkwater (1996).

Cochrane et al. (2000) speculated that the ecology of Emerald Basin "…may constitute an effective barometer of the health of the surrounding Scotian Shelf and bank areas." and proceeded to extend relevant Basin time series to euphausiids and pelagic fish to further explore this concept. Emerald Basin does appear to constitute an area of accumulation for *C. finmarchicus* during the summer months and its depths provide a relatively undisturbed repository for mature developmental stages of the same during the winter months. These overwintering Calanus, in turn, likely boost Basin copepod abundances during the following spring (Herman et al. 1991; Sameoto and Herman 1990). High Basin copepod populations could trigger enhanced Basin euphausiid productivity one trophic level higher. Might enhanced euphausiid biomasses in Emerald Basin also contribute to the euphausiid biomasses observed over wider Scotian Shelf areas, especially those of the western shelf which we have seen generally displays higher euphausiid populations than the eastern shelf for reasons not fully understood? We also speculate that euphausiids may be advectively transported from the usually euphausiid-rich Slope areas through the deeper regions of Emerald and LaHave Basins to augment populations in the surrounding shelf areas. The ADCP backscatter time series of Fig. 16 could be interpreted as consistent with an Emerald

[12] Trends in the post-1994 *C. finmarchicus* abundances (Fig. 6) appear more definite than those for *M. norvegica* in the same figure, the number of samples per survey for the former being higher.

Basin primacy in determining wider shelf euphausiid abundances. While backscatter trends prior to fall 2001 appear different for both the eastern and western Scotian Shelves (generally upward) compared to Emerald Basin (nearly constant or slightly downwards), backscatter levels in Emerald Basin on broad time average are, we have also noted, a factor of ~2 higher than those on the western Scotian Shelf and a factor of ~4 higher than those on the eastern shelf – at least before the simultaneously and precipitous population drop in fall 2001. The suggestive positive correlation (both visual and computed) between 200 kHz Emerald Basin euphausiid populations and deep Basin temperatures (Fig. 19) could be interpreted as consistent with occasional influxes at depth of warm euphausiid-rich slope water into the Shelf Basins.

The sharp transition from relatively high ADCP backscatter levels prior to late 2001 to the markedly lower values persisting to late 2004 (end of ADCP data) for all three shelf regions would again argue for systematic coupling between all three shelf regions. The fact that the independent DataSonics 200 kHz deep Emerald Basin backscatter measures of Fig. 10 displayed a corresponding dip in unsmoothed backscatter, similarly initiating in the fall of 2001 and persisting until early 2004, strongly argues that the ADCP level transitions for Emerald Basin and the wider shelf regions constitute more than calibration artefacts, a conclusion also supported by our earlier (section 3.5.) linear regression of decibel ADCP levels against same survey decibel 200 kHz levels (Figs. 14 and 15).

4.5. BROAD SCALE CORRELATES

Any NAO influences on Scotian Shelf ecosystems could be both lagged and diffused in time if, for example, the thermal effects of an NAO-altered Labrador Current must be advected from afar rather than the NAO influence being exerted locally and almost immediately (Petrie 2007; Drinkwater 1996; Drinkwater and Gilbert 2004; Hakkinen and Rhines 2009; Wang et al. 2016). Petrie (2007) reported a significant positive correlation between deep (250 m) Emerald Basin temperatures and the Winter NAO index anomaly, the correlation improving when the NAO anomalies were causally summed for intervals up to 5 years. On low NAO **winter** anomaly years, enhanced outer shelf edge Labrador Current transport triggered not infrequent incursions of very cold Slope waters, containing a high Labrador Current mixed fraction, into the deep inner Shelf Basins and into adjacent deep central and western Scotian Shelf areas. In contrast, eastern continental shelf water temperatures negatively correlated with the NAO, a direct influence of the warmer winter air temperatures accompanying low NAO winter anomaly years, with comparatively little influence from the Slope region.

The 5-year **causal** smoothed NAO index (Fig. 20) displayed a steady rise from about 1980 to 1993 coincident with a period of generally rising 200 kHz backscatter levels in Emerald Basin (Fig. 10).[13] The observed 1994-95 peak in 200 kHz Emerald Basin backscatter

[13] The NAO smoothed curve of Fig. 20 is displaced forward in time by 2.5 years (1/2 of the 5 year running mean smoothing interval) compared to the unsmoothed time series, whereas polynomial fits to the 200 kHz S_a time series are not systematically shifted in time. Therefore, an observed direct visual correlation of these two quantities as graphically presented without corrective time shifts might suggest a 2 – 3 year lag between NAO related atmospheric forcing and any consequent biological response.

roughly corresponds with peak deep Basin temperatures, the culmination of a long warming trend starting about 1965 (Drinkwater et al. 2003) and consistent with our own survey temperature data (Fig. 18) covering the latter portions of this temperature rise. In the post-peak period, backscatter levels (Fig. 10) declined in an irregularly manner to the 2011 data termination. Emerald Basin bottom temperatures also declined slightly but were interrupted by two limited-duration cold events discussed below. The early to mid-1990s also marked the beginning of a long term transition from highly positive to highly negative anomalies both in the regular and in the winter (Dec - Mar) NAO indices (Drinkwater 1996; Hurrell and NCAR Staff 2016). The 5-yr **causal** NAO index (Fig. 20) exhibited an overall downward trend from about 1994 to 2011 with a further broad dip centered in 1999 originating from a period of low monthly indices extending from about 1995 to the end of 1998. This period culminated in an oceanographic cold event initiating in December 1997 when very cold Labrador Slope water flooded Emerald Basin and deeper areas of the broader Scotian Shelf, the cold waters persisting in the deeper portions of Emerald Basin through 1998 into 1999 (Drinkwater et al. 2003). This cold event was **not** accompanied by a clear signature in our Emerald Basin 200 kHz backscatter. A second, longer duration deep Emerald Basin cold event (Fig. 18) was observed in the fall of 2007 and persisted to the end of 2009. The longer event, in contrast, was accompanied by (fall 2007) the lowest 200 kHz backscatter levels observed during the entire course of our Emerald Basin observations, the backscatter recovering by the spring of 2010.

The fall 2001 profound dip in Emerald Basin backscatter appeared unrelated to deep Basin temperatures, s_a values remaining low through the fall of 2003 (Figs. 10 and 16). Both the eastern and western Scotian Shelves were also similarly affected (Fig. 16), all backscatter levels recovering to a degree in 2003. Interestingly, about year 2001 marked the initiation of a major westward shift and expansion of the peripheral circulations of the North Atlantic sub-polar gyre lasting until at least 2007 (Hakkinen and Rhines 2009; Wang et al. 2009). The latter investigators modelled a steady intensification through years 2000 – 2002 of, particularly, the western branch of the Labrador Current whose southern extension potentially affects the Scotian Shelf. The fall 1997 Scotian Shelf cold event was preceded by a high spike in winter 1996-97 (west) Labrador Current speeds upstream on Hamilton Bank (55º 7' N 54º 7'W) and a negative spike in the 1996 NAO winter index (Wang et al. 2016). Similarly, the later fall 2007 Emerald Basin cold event was preceded by another spike in measured Hamilton Bank flow in the winter of 2006-07 and increasingly negative winter NAO indices through 2004 – 06. While a negative spike in the NAO index occurred at the time of the apparent reorganization of the northern gyre circulation (2001), and was also accompanied by an enhancement of Hamilton Bank flow observed during 2002 (using Wang et al.'s presented data), this reorganization appeared not to provoke an immediate Shelf Basin cold event. Therefore, if the inferred 2001 drop in Scotian Shelf (including Emerald Basin) euphausiid biomass was real and had some connection to the gyre reorganization, it appeared mediated by processes apart from a cold water influx at depth in Emerald Basin.

The physical/biological factors responsible for the apparent CPR-delineated broad but modest **dips** in smoothed euphausiid abundances on the western and entire Scotian Shelves

during the mid-to-late 1990s and subsequent abundance rises to about year 2001, the rises being roughly consistent with the observed ADCP backscatter trends (both eastern and western Scotian Shelves), remain unknown. The same fundamental lack of understanding marks the contrasting **peak** in Emerald Basin euphausiid backscatter abundances in in the mid-1990s followed by an overall decline to 2001 (most reliably indicted by the 200 kHz data) although we have noted some correspondence between long term trends in euphausiid abundance, deep Basin temperatures, and high NAO indices. The cause of the marked decline in euphausiid abundances in Emerald Basin (200 kHz and ADCP) starting in the fall of 2001 and the simultaneous almost order of magnitude population declines on the eastern and western Scotian Shelves (ADCP) is unknown. While non-biological explanations involving an anomalous shift in instrumental calibration are quite possible for the ADCP data, the simultaneous drop in the instrumentally unrelated 200 kHz Emerald Basin backscatter does support its reality. While no clearly analogous long-term dip occurs in the CPR euphausiid populations (factor of ~10 seasonal fluctuations are present) CPR counts are dominantly larval whereas backscatter is dominated by adults. Nevertheless, some distinctive signature in the CPR counts might have been anticipated; future analysis of 200 kHz backscatter data for the wider shelf could elucidate this puzzle.

In summary, the preponderance of evidence from a variety of sampling techniques is that euphausiid populations, apart from seasonal fluctuations related to their life cycles, do fluctuate systematically on time scales from yearly to decadal or longer. Basic ecological studies are still required to understand why euphausiids possessing a life span of 1 to 3 years display these longer population fluctuations. While functional correlations between euphausiid abundances and long-term trends in deep Shelf Basin temperatures, or with NAO indices, etc. are highly suggestive we do not propose definitive causal hypotheses. Some changes may well be related to Labrador Current transport fluctuations. Any biological variations at the longest 30 – 40 year multi-decadal time scales examined could be influenced by global warming. Profound changes in Scotian Shelf oceanography and biology did occur during the course of our macrozooplankton studies. Especially noteworthy is the collapse of demersal fish species on the eastern Scotian Shelf, including the Atlantic cod (*Gadis morhua*), a decline pronounced by the early 1990's but initiating in the mid-1980's or even earlier (Zwanenburg et al. 2002; Choi et al. 2004).[14]

5. RECOMMENDATIONS

Several recommendations are advanced to facilitate and to extend the types of studies covered by this report:

1) A wider recognition of the unique value of extended biological time series: The requirement for long biological time-series at the lower and intermediate trophic levels of marine ecosystems is especially critical for:

- Reliable separation of and accurate characterization of both short term natural ecosystem variability and longer term trends

[14] We make no direct causal implication between the decline of demersal fish stocks and fluctuations in macrozooplankton abundances although common factors may have influenced both phenomena.

- The delineation of primary ecosystem processes and dependencies using long-duration multivariate correlation studies between differing biological components and potential natural or anthropogenic origin ecosystem stressors including, at the longest time scales, climate change
- Providing quantitative, observation-based biological inputs to, and placing real observational performance constraints on, multi-trophic level ecosystem models
- Evidence-based exploration of the efficacies of establishing and maintaining Marine Protected Areas

2) A better recognition of the peculiar financial and technical resources required for the production of reliable extended time series. The scientific value of multi-decadal zooplankton and macro-zooplankton time series, frequently sampled, properly calibrated, and utilizing standardized methodologies is often not fully appreciated at monitoring inception. This can make justification of necessary resources particularly difficult within short-term targeted funding environments. In addition, the generation of long biological time series using specialized measurement technologies like acoustic backscatter involves complex instrumentation, challenging calibration methodologies, and informed data reduction. Success requires high level support from personnel with the requisite technical know-how and instrument-specific expertise which must be maintained in continuity over multi-decade time spans in spite of rapid technological evolution, inevitable program and institutional reorganizations, and staff turnovers. This mandates that the long-term objectives and necessary resource allocations be well understood and supported at higher management levels. At the operational level, acquired data sets should be **quickly** reduced to standardized, permanent, and easily accessible archival forms with all necessary supportive documentation for future generations of researchers. The abilities to accurately reduce acquired data sets to standardized measures and to correctly harmonize data sets collected with variant hardware and evolving protocols quickly disappear with elapsed time. Time can even obscure knowledge of the existence of relevant data sets – therefore, the necessity of an integrated parallel, well-coordinated institutional data management plan.

3) At the scientific level, both the spatial/temporal sampling problem and the biases inherent in tracking underlying populations using size or otherwise selective macro-zooplankton sampling techniques must be better understood.

4) In regard to future data collection strategies, any temporal under-sampling in macrozooplankton acoustic backscatter measures resulting from the current semi-annual surveys might be effectively explored and at least partially addressed by using permanent bottom-mounted or deep-moored multiple frequency echosounders installed at strategically chosen Scotian Shelf locations such as central Emerald Basin and Roseway Basin on the western shelf, and possibly within the Gully MPA on the eastern shelf. As of 2017, the required technology is available off-the-shelf and promises high quantitative performance and long endurance at modest costs. If improved spatial coverage is also deemed essential then emerging technologies such as gliders equipped with backscatter systems – even low power and short-range - might provide alternative paths forward.

5) A large collection of geo-referenced 200 kHz backscatter data for the wider Scotian Shelf presently exists and may be suitable for future macrozooplankton studies. However, the necessity of applying after-the-fact acoustic absorption corrections and, especially, significant corrections for transducer temperature (usually not required for more modern backscatter systems) would make precise quantification tedious.

6. ACKNOWLEDGEMENTS

Many have contributed to this work. Most individuals assisting with the earlier phases have been acknowledged in prior publications. The Sir Alister Hardy Foundation for Ocean Science, both institution and staff, are especially acknowledged for making the historical (earlier sampling period) portion of their Scotian Shelf Continuous Plankton Recorder database available to DFO and for their provision of valuable supporting advice. The Ocean Physics Section, of DFO's Ocean Sciences Division, and especially Murray Scotney, are thanked for their able long-term handling of the ADCP system and its associated data streams. More recently Jeff Spry, Scott Young, and Randy King of BIO's Ocean Sciences Division performed the laborious but necessary survey-specific acoustic transducer installations on CCGS HUDSON. Erica Head and Ed Horne served as Senior Scientists on multiple AZMP monitoring surveys in the critical post-1996 to 2011 period during which multi-frequency acoustic backscatter data was collected as an unfunded supplement to core AZMP programs. During this latter period we also acknowledge the efficient cooperation and professionalism of the officers and crew of CCGS HUDSON.

Detailed critiques of earlier versions this manuscript by Brian Petrie and Catherine Johnson have been immensely helpful in preparation of the final product and their help is gratefully acknowledged. However, the authors should make clear that the reviewers served in an advisory capacity only and that the report's contents should neither be considered as necessarily reflecting their views nor as necessarily carrying their full endorsement.

Earlier portions of this work have been funded in part by the Canadian GLOBEC program. In manuscript preparation, taxonomic reference has been made to the World register of marine species (WoRMS), accessed online: http://www.marinespecies.org.

7. REFERENCES

Calise, L., and Skaret, G. 2011. Sensitivity investigation of the SDWBA Antarctic krill target strength model to fatness, material contrast and orientation. CCAMLR Sci. 18: 97–122.

Choi, J.S., Frank, K.T., Leggett, W.C., and Drinkwater, K. 2004. Transition to an altered state in a continental shelf ecosystem. Can. J. Fish. Aquat. Sci. 61: 505-510.

Choi, J.S., Frank, K.T., Petrie, B.D., and Leggett, W.C. 2005. Integrated assessment of a large marine ecosystem: A case study of the devolution of the eastern Scotian Shelf, Canada. *In* Oceanography and marine biology: An annual review. Vol. 45. Edited by R.N. Gibson, R.J.A. Atkinson, and J.D.M. Gordon. CRC Press, Boca Raton. pp. 47-67 + Figs.

Clay, C.S., and Medwin, H. 1977. Acoustical oceanography: Principles and applications. John Wiley and Sons, New York. 544 p.

Cochrane, N.A., and Sameoto, D.D. 1987. Multichannel false color echograms as a biological interpretative tool. *In* Progress in underwater acoustics. Edited by. H.M. Merklinger. Plenum Press, New York. pp. 129-135.

Cochrane, N.A., Sameoto, D., Herman, A.W., and Neilson, J. 1991. Multiple-frequency acoustic backscattering and zooplankton aggregations in the inner Scotian Shelf basins. Can. J. Fish. Aquat. Sci. 48: 340-355.

Cochrane, N.A., Sameoto, D.D., and Belliveau, D.J. 1994. Temporal variability of euphausiid concentrations in a Nova Scotia shelf basin using a bottom-mounted acoustic Doppler current profiler. Mar. Ecol. Prog. Ser. 107: 55–66.

Cochrane, N.A., Sameoto, D.D., and Herman, A.W. 2000. Scotian Shelf euphausiid and silver hake population changes during 1984 – 1996 measured by multi-frequency acoustics. ICES J. Mar. Sci. 57: 122–132.

Demer, D.A., and Conti, S.G. 2003. Reconciling theoretical versus empirical target strengths of krill: Effects of phase variability on the distorted-wave Born approximation. ICES J. Mar. Sci. 60: 429–434.

Drinkwater, K.F. 1996. Atmospheric and oceanic variability in the Northwest Atlantic during the 1980s and early 1990s. J. Northw. Atl. Fish. Sci. 18: 77 – 97.

Drinkwater, K.F. and Gilbert, D. 2004. Hydrographic variability in the waters of the Gulf of St. Lawrence, the Scotian Shelf and the Eastern Gulf of Maine (NAFO Subarea 4) during 1991 – 2000. J. Northw. Atl. Fish. Sci. 34: 83 – 99.

Drinkwater, K.F., Petrie, B., and Smith, P.C. 2003. Climate variability on the Scotian Shelf during the 1990s. ICES Mar. Sci. Symp. 219: 40 – 49.

Foote, K.G. 1990. Target strengths of Antarctic krill (*Euphausia superba*) at 38 and 120 kHz. J. Acoust. Soc. Am. 87: 16–24.

Francois, R.E., and Garrison, G.R. 1982a. Sound absorption based on ocean measurements: Part I: Pure water and magnesium sulfate contributions. J. Acoust. Soc. Am. 72(3): 896-907.

Francois, R.E., and Garrison, G.R. 1982b. Sound absorption based on ocean measurements: Part II: Boric acid contribution and equation for total absorption. J. Acoust. Soc. Am. 72(6): 1879-1890.

Greenlaw, C.F., and Johnson, R.K. 1982. Physical and acoustical properties of zooplankton. J. Acoust. Soc. Am. 72(6): 1706-1710.

Hakkinen, S. and Rhines, P.B. 2009. Shifting surface currents in the northern North Atlantic Ocean. J. Geophys. Res. C04005, doi:10.1029/2008JC004883.

Herman, A.W., Sameoto, D.D., Chen, Shunnian, Mitchell, M.R., Petrie, B., and Cochrane, N.A. 1991. Sources of zooplankton on the Nova Scotia Shelf and their aggregations within deep shelf basins. Continental Shelf Research 11(3): 211 – 238.

Hurrell, J. and National Center for Atmospheric Research Staff (Eds.) 2016. The climate data guide: Hurrell North Atlantic Oscillation (NAO) index (station-based). https://climatedataguide.ucar.edu/climate-data/hurrell-north-atlantic-oscillation-nao-index-station-based (accessed 15 Sept. 2016).

Køgeler, J.W., Falk-Petersen, S., Kristensen, Å., Pettersen, F., and Dalen, J. 1987. Density and sound speed contrasts in sub-Arctic zooplankton. Polar Biology 7: 231-235.

Kristensen, Å. and Dalen, J. 1986. Acoustic estimation of size distribution and abundance of zooplankton. J. Acoust. Soc. Am. 80(2): 601-611.

Kubilius, R., Ona, A., and Calise, L. 2015. Measuring *in situ* krill tilt orientation by stereo photogrammetry: examples for *Euphausia superba* and *Meganyctiphanes norvegica*. ICES J. Mar. Sci. 72(8): 2494 – 2505.

Mackenzie, K.V. 1981. Nine-term equation for sound speed in the oceans. J. Acoust. Soc. Am. 70: 807-812.

McQuinn, I.H., Reid, D., Berger, L., Diner, N., Heatley, D., Higginbottom, I., Anderson, L.N., Langeland, O., and Lapierre, J.P. 2005. Description of the ICES *HAC* Standard Data Exchange Format, version 1.60. ICES Cooperative Research Report No. 278: 86 pp.

Novarini, J.C., Keiffer, R.S., and Norton, G.V. 1998. A model for variations in the range and depth dependence of the sound speed and attenuation induced by bubble clouds under wind-driven sea surfaces. IEEE J. Oceanic Eng. 23(4): 423-438.

NWS Climate Prediction Center. 2014. Monthly mean NAO index since January 1950. http://www.cpc.ncep.noaa.gov/products/precip/CWlink/pna/norm.nao.monthly.b5001.current.ascii (accessed 09 June 2014).

Petrie, B. 2007. Does the North Atlantic Oscillation affect hydrographic properties on the Canadian Atlantic continental shelf? Atmos.-Ocean 45(3): 141 – 151.

Petrie, B. and Drinkwater, K. 1993. Temperature and salinity variability on the Scotian Shelf and in the Gulf of Maine 1945 – 1990. J. Geophys. Res. 98: 20079-20089.

RD Instruments. 1990. Calculating absolute backscatter. Technical Bulletin ADCP-90-04, Dec. 1, 1990. 24 p.

RD Instruments. 1991. Vessel-mounted acoustic Doppler current profiler (VM-ADCP) Technical Manual (Sept. 1991). RD Instruments, 9855 Business Park Ave., San Diego, CA 92131.

Sameoto, D.D. 1980. Quantitative measurements of euphausiids using a 120-kHz sounder and their in situ orientation. Can. J. Fish. Aquat. Sci. 37: 693-702.

Sameoto, D. 2001. Decadal changes in phytoplankton color index and selected calanoid copepods in continuous plankton recorder data from the Scotian Shelf. Can. J. Fish. Aquat. Sci. 58: 749-761.

Sameoto, D. and Cochrane, N. 1996. Euphausiids on the eastern continental shelf. DFO Atlantic Fish. Res. Doc. 96/119: 12 p.

Sameoto, D.D. and Herman, A. 1990. Life cycle and distribution of *C. finmarchicus* in deep basins on the Nova Scotia shelf and seasonal changes in Calanus spp. Mar. Ecol. Prog. Ser. 66: 225–237.

Sameoto, D.D., Jaroszynski, L.O., and Fraser, W.B. 1980. BIONESS: A new design in multiple net zooplankton samplers. Can. J. Fish. Aquat. Sci. 37: 722-724.

Sameoto, D., Cochrane, N.A., and Herman, A.W. 1985. Response of biological acoustic backscattering to ships' lights. Can. J. Fish. Aquat. Sci. 42(9): 1535-1543.

Sameoto, D., Cochrane, N., and Herman, A. 1993. Convergence of acoustic, optical, and net-catch estimates of euphausiid abundance: Use of artificial light to reduce net avoidance. Can. J. Fish. Aquat. Sci. 50: 334-346.

Sameoto, D. Kennedy, M.K., and Cochrane, N. 1997. Zooplankton changes along the Halifax and Louisbourg transects in 1996. DFO Can. Stock Assess. Sec. Res. Doc. 97/82: 14 p.

Sameoto, D., Cochrane, N., Herman, A., Head, E., and Kennedy, M.K. 1998. State of zooplankton on the Scotian Shelf, 1997. DFO Can. Stock Assess. Sec. Res. Doc. 98/130: 29 p.

Simard, Y., McQuinn, I., Montminy, M., Lang, C., Miller, D., Stevens, C., Wiggins, D., and Marchalot, C. 1997. Description of the *HAC* standard format for raw and edited hydroacoustic data, version 1.0. Can. Tech. Rep. Fish. Aquat. Sci. 2174: Vii + 65 pp.

Stanton, T.K., Clay, C.S., and Chu, D. 1993. Ray representation of sound scattering by weakly scattering deformed fluid cylinders: Simple physics and application to zooplankton. J. Acoust. Soc. Am. 94(6): 3454–3462.

Stanton, T.K., Chu, D., and Wiebe, P.H. 1996. Acoustic scattering characteristics of several zooplankton groups. ICES J. Mar. Sci. 53: 289-295.

Thorpe, S.A. 1992. Bubble clouds and the dynamics of the upper ocean. Q. J. R. Meteorol. Soc. 118: 1-32.

Tichy, F.E., Solli, H., and Klaveness, H. 2003. Non-linear effects in a 200-kHz sound beam and the consequences for target-strength measurement. ICES J. Mar. Sci. 60: 571–574.

Wang, Z., Brickman, D., Greenan, B.J.W., and Yashayaev, I. 2016. An abrupt shift in the Labrador Current system in relation to winter NAO events. J. Geophys. Res. 121: 5338 – 5349, doi:10.1002/2016JC011721.

Wiebe, P.H., Lawson, G.L., Lavery, A.C., Copley, N.J., Horgan, E., and Bradley, A. 2013. Improved agreement of net and acoustical methods for surveying euphausiids by mitigating avoidance using a net-based LED strobe light system. ICES J. Mar. Sci. 70(3): 650-664.

Worcester, T. and Parker, M. 2010. Ecosystem status and trends report for the Gulf of Maine and Scotian Shelf. DFO Can. Sci. Advis. Sec. Res. Doc. 2010/070: vi + 59 p.

Zedel, L., and Farmer, D. 1991. Organized structures in subsurface bubble clouds: Langmuir circulation in the open ocean. J. Geophys. Res. 96(C5): 8889-8900.

Zwanenburg, K.C.T., Bundy, A., Strain, P., Bowen, W.D., Breeze, H., Campana, S.E., Hannah, C., Head, E., and Gordon, D. 2006. Implications of ecosystem dynamics

for the integrated management of the Eastern Scotian Shelf. Can. Tech. Rept. Fish. Aquat. Sci. 2652: xiii + 91 p.

Zwanenburg, K.C.T., Bowen, D., Bundy, A., Drinkwater, K., Frank, K. O'Boyle, R., Sameoto, D., and Sinclair, M. 2002. Decadal changes in the Scotian Shelf large marine ecosystem. *In*: Large Marine Ecosystems of the North Atlantic: changing states and sustainability. Edited by K. Sherman and H.R. Skjoldal. Elsevier Science B.V., Amsterdam. pp. 105 – 150.

TABLES

Table 1. Most commonly utilized vertical beam echosounder operational parameters.

Freq kHz	Transducer Type	Beamwidth º -3 dB to +3 dB	Pulse Length ms	Passband kHz	Output Power Nominal kW
12	EDO – 323B	35	2	1	0.4
50	Furuno 50B-12	18	2	1	0.4
122	Simrad 68BA	10	2	1	1
200	Furuno 200B-8	5.4	5	1	2

Table 2. Parameters utilized in the computation of volume backscattering strength from ADCP raw echo counts.

Quantity	Numerical Value	Units	Definition
c	1486.65[1]	m/s	Speed of sound over profile
α	0.042[1]	dB/m	Sound absorption coefficient over profiling range
ξ	30	º	Beam angle from vertical
d	6 or 4.8	M	Depth of transducer face
T_{EC}	19.00	ºC	Temp. of system electronics during calibration
T_E	19.0	"	Temp. of system electronics in field
T_{XC}	10.10	"	Temp. of transducer during calibration
T_X		"	Temp. of transducer in field (recorded real-time)
E		Counts	Echo intensity in field (recorded real-time)
$E_{RC}[ibeam]$	Beam 1: 31 2: 34 3: 37 4: 34	Counts	Beam-specific reference thermal noise of electronics during calibration
$E_R[ibeam]$		Counts	Real-time reference level for echo intensity (counts) computed as below:
Computation of $E_R[ibeam]$	Calculate : $A \times E_{RC}[ibeam] + (1.0 - A)(292.0 + 0.133\ T_E) + (1.0 - B)(27.3 + 0.1\ T_X)$ where $A = (T_E + 273.0) / (T_{EC} + 273.0)$ $B = (T_X + 273.0) / (T_{XC} + 273.0)$		
$K_1[ibeam]$		W	Beam-specific power into water corrected for real-time transmit voltage, computed as below:
Computation of $K_1[ibeam]$	Calculate: $K_1 = [\ ((V_s \times 1.397) - 4.27) / 37.14]^{\ 2} \times K_{1c}$		
$K_{1c}[ibeam]$	Beam 1: 5.81 2: 5.88 3: 5.52 4: 5.60	W	Beam-specific nominal power into water; constant supplied by manufacturer
$K_2[ibeam]$	Beam 1: 2.72 2: 2.59 3: 2.57 4: 2.20	W	Beam-specific system noise factor; constant supplied by manufacturer
K_c	0.43	dB/cnts	Conversion factor for echo intensity

			K_c = 127.3 / (T_E + 273.0) converts ADCP echo intensity from counts to dB before absorption and beam spreading corrections.
K_s	4.17 x 10^5	/m^2s	System constant (depends on ADCP frequency) Ratio of system bandwidth to the square of the transducer diameter
Bin Width	4	M	Depth cell length; selects the volume of water for one measurement cell
Pulse Length	4	M	Transmit pulse length (usually set to equal depth cell length)
Delay	2	M	Blank after transmit (gives transducer time to recover after transmit)
Ibeam	1 – 4		Beam number
Ibin			Depth cell (bin) number of the scattering layer being measured
R		M	Slant range along beam to depth cell; computed from specified system parameters as below:
Computation of *R*	Calculate: ((*Delay* + (*ABS*(*Pulse Length* – *Bin Width*) / 2) + (*ibin* x *Bin Width*) + (*Bin Width* / 4)) / *cos*(ζ)) (*c* / 1475.1)*		
V_s		V	Real-time transmit voltage (recorded real-time)

[1] Calculated for each survey and area.

Note: At the hardware level, instrument delays, pulse widths, and bin widths are defined in the time domain and are related to spatial scales in the vertical direction assuming a nominal sound speed of 1475.1 m/s. The ratio of real-time sound speed, c, to the nominal value is used as a fine correction factor in computing precise slant range. Echo intensity is sampled in the lower ¼ of each depth bin.

Table 3. Model-derived effective target strengths of a 2.8 cm *M. norvegica* ensonified by a narrow vertical beam 200 kHz echosounder for several average organism tilt angles to the vertical and tilt standard deviations about the average tilt, all defined in 3-D space. More probable values are entered in bold type. The effects of 2-D as opposed to 3-D distribution functions are entered in blue italics. Acoustic parameters are density ratio g = 1.05 and sound speed ratio h = 1.03.

	3-D Standard Deviation º					
Ave. Tilt º	**0**	**10**	**20**	**30**	**40**	**Random**
0	-63.9	-69.5	-72.3	-73.9	-75.1	-75.7
10	-77.9	-71.4	**-72.8** ***-72.5***	**-74.2** ***-73.6***	**-75.2** ***-74.2***	
20	-81.6	-76.9	**-74.3** ***-73.8***	**-74.8** ***-74.1***	**-75.5** ***-74.5***	
30	-87.1	-84.1	**-76.8** ***-76.0***	**-75.9** ***-74.9***	**-76.1** ***-74.8***	
40	-91.6	-89.0	-80.2	-77.4	-76.8	

Table 4. Model-derived effective target strengths of a random azimuthally oriented 2.8 cm *M. norvegica* ensonified by a 30º inclined beam 153.4 kHz ADCP for several average organism tilt angles to the vertical and tilt standard deviations about the average tilt, all defined in 3-D space. More probable values are entered in bold type. The effects of 2-D as opposed to 3-D distribution functions are entered in blue italics. Acoustic parameters are density ratio g = 1.05 and sound speed ratio h = 1.03.

	3-D Standard Deviation º					
Ave. Tilt º	**0**	**10**	**20**	**30**	**40**	**Random**
0	-73.0	-72.7	-72.4	-73.1	-73.8	-74.2
10	-72.7	-72.3	**-72.5** ***-72.4***	**-73.2** ***-72.8***	**-73.8** ***-73.2***	
20	-71.7	-71.9	**-72.9** ***-72.7***	**-73.6** ***-73.1***	**-74.1** ***-73.3***	
30	-70.5	-72.7	**-73.8** ***-73.3***	**-74.2** ***-73.4***	**-74.5** ***-73.5***	
40	-84.7	-76.0	-75.3	-75.1	-75.0	

Table 5. Species of euphausiid identified in samples collected on the AZMP stations.

Euphausiid species	**Percentage of total euphausiids collected**
Thysanoessa longicaudata	35.2
Meganyctiphanes norvegica	31.4
Thysanoessa inermis	13.5
Nematoscelis megalops	4.3
Euphausia krohni	3.7
Thysanoessa raschi	1.5
Stylocheiron elongatum	0.7
Stylocheiron maximum	0.4
Nyctiphanes couchi	0.3
Bentheuphausia amblyops	0.1
Thysanopoda acutifrons	0.1
Thysanopoda microphthalm	0.1
Euphausia eximia	0.01

Table 6. Relative abundances of taxonomic groups for animals > 1 cm in length.

Taxonomic group	**Percentage of total animals collected**
Euphausiids	35.5
Chaetognaths	27.6
Fish larvae	7.9
Amphipods	5.7
Mysids	4.9
Salps	4.8
Decapods	2.7

Table 7. Concerning 200 kHz acoustic backscatter data processed for each individual survey: The number of analysed data subsections characterized by slow vessel speeds (1.5 ms^{-1}), denoted "BIONESS TYPE", and by faster vessel speeds (4.5 ms^{-1}), denoted "BATFISH TYPE".

YEAR	MONTH	BIONESS TYPE	BATFISH TYPE
1984	10	1	2
1985	6	1	
1986	9	5	2
1987	NONE		
1988	6	3	2
1989	10	1	1
1990	5	2	1
	10	3	1
1991	10	4	2
1992	11	5	2
1993	5		1
1994	5	3	1
	6	2	1
1995	4	3	1
	10		1
1996	6	2	2
	11	3	
1997	4	2	1
	10	3	2
1998	4	3	6
	10	2	1
1999	4	1	1
	10	4	2
2000	10	7	3
2001	5	1	8
	10		2
2002	10		4
2003	4	1	2
	10	2	1
2004	4	2	6
2005	10	1	2
2006	5	4	6
2007	10	2	3
2008	4		2
	10	2	2
2009	4	1	3
	10	1	1
2010	4	1	1
2011	4	2	

FIGURES

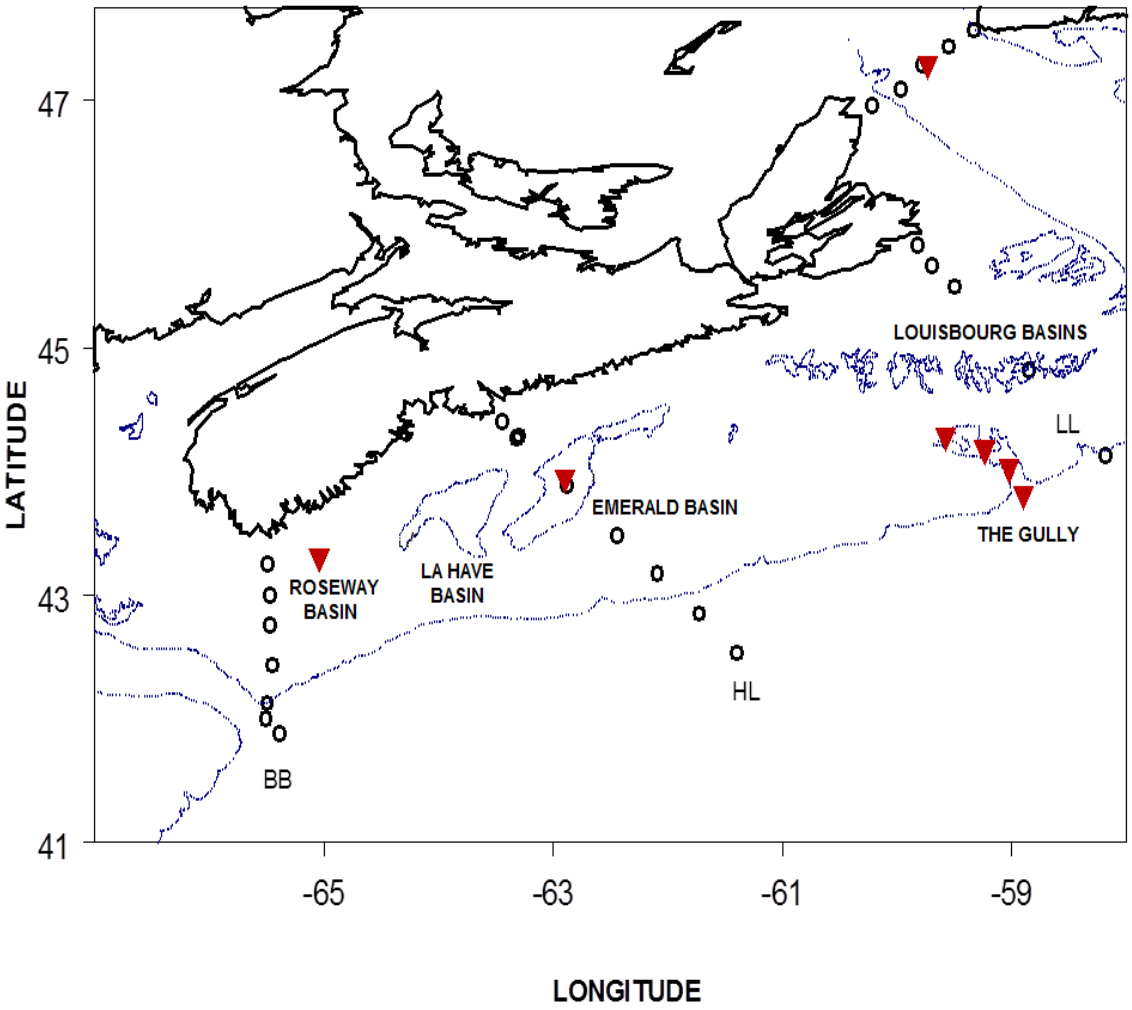

Figure 1. AZMP plankton net sampling stations on the Scotian Shelf. Triangles represent stations on which samples were taken with the BIONESS and circles represent stations on which vertical ring net tows were taken. BB – Browns Bank line, HL – Halifax line, LL – Louisbourg line.

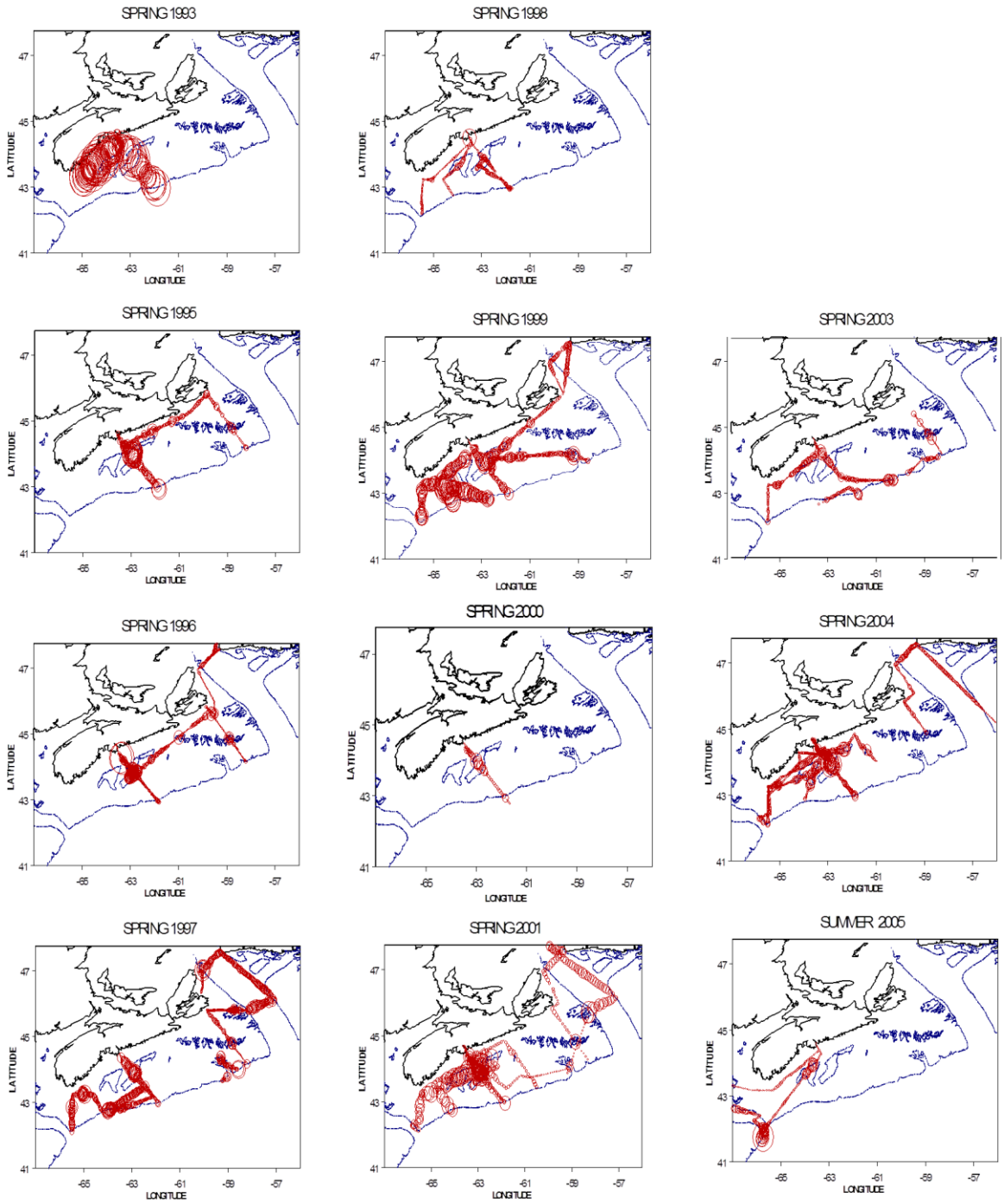

Figure 2. ADCP-derived water column sa for spring periods. Larger red circles correspond to higher sa values.

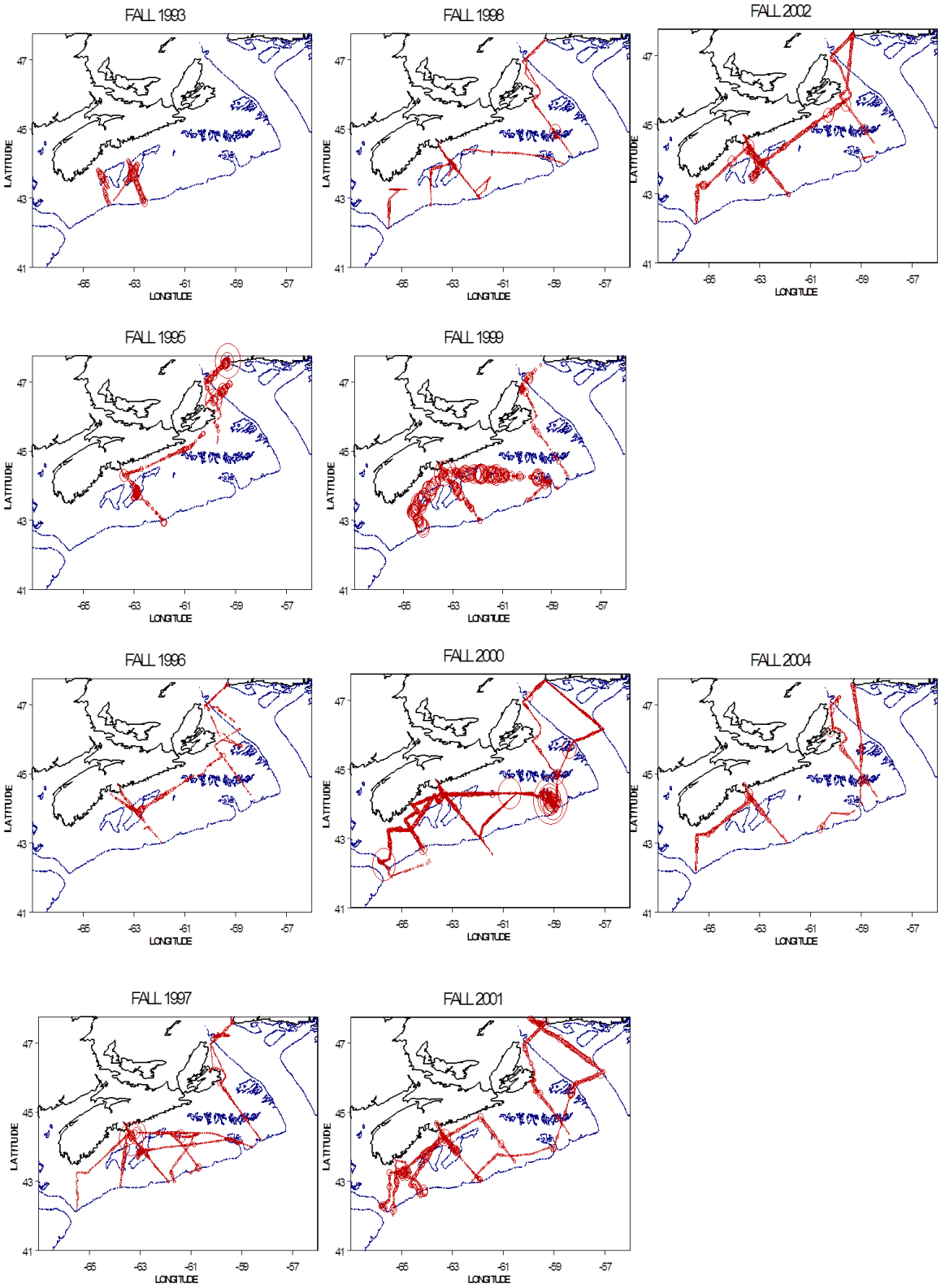

Figure 3. ADCP-derived water column s_a for fall periods. Larger red circles correspond to higher s_a values.

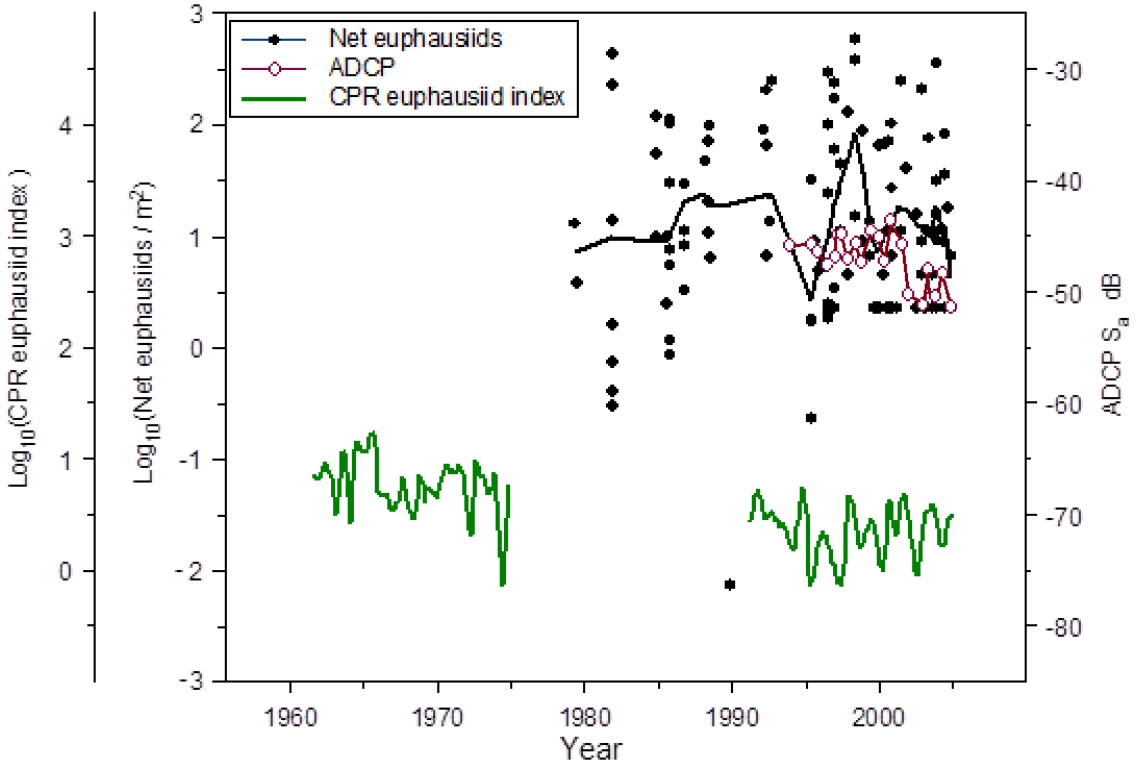

Figure 4. Log_{10} values for both the CPR euphausiid index (no. of euphausiids per sample) and the no. of euphausiids per m^2 from net samples, and ADCP S_a, each quantity plotted vs. time for the western Scotian Shelf. The lines are least-squares fitted Kernel smoothers.

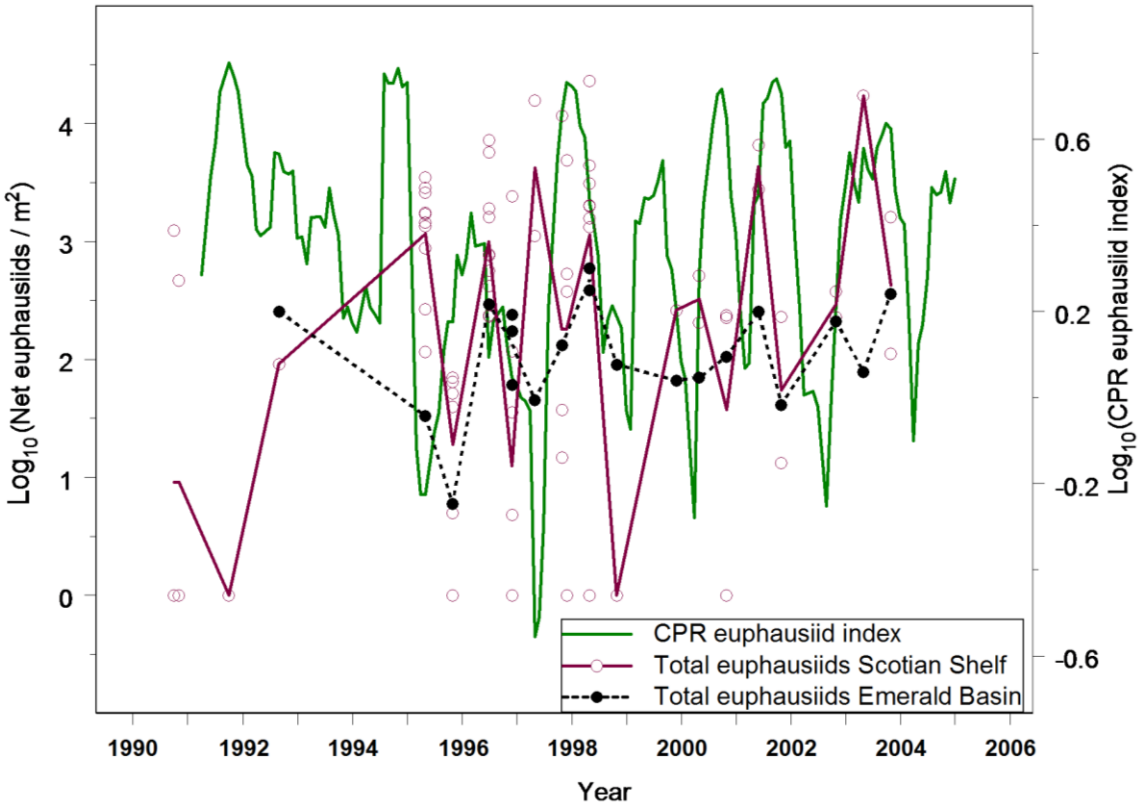

Figure 5. Log_{10} values for mean column number of euphausiids collected with the BIONESS for both the entire Scotian Shelf and for Emerald Basin plus the CPR logarithmic euphausiid index for the entire Scotian Shelf, all plotted vs. time. The lines are least-squares fitted Kernel smoothers. Note that the LHS and RHS logarithmic scales differ.

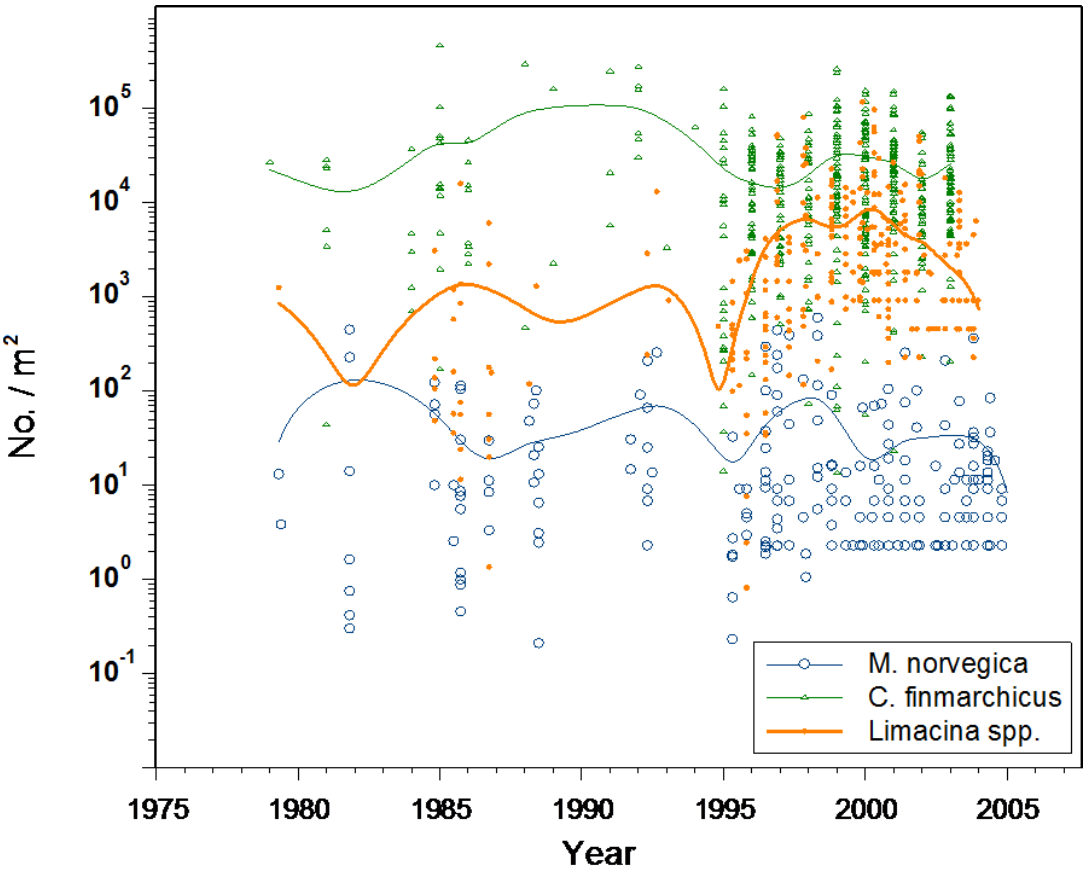

Figure 6. Mean column numbers of three zooplankters on the Scotian Shelf contributing to ADCP acoustic backscattering obtained by net sampling. Lines are least-squares cubic spline smoothers but data are quite sparse and scattered prior to 1995.

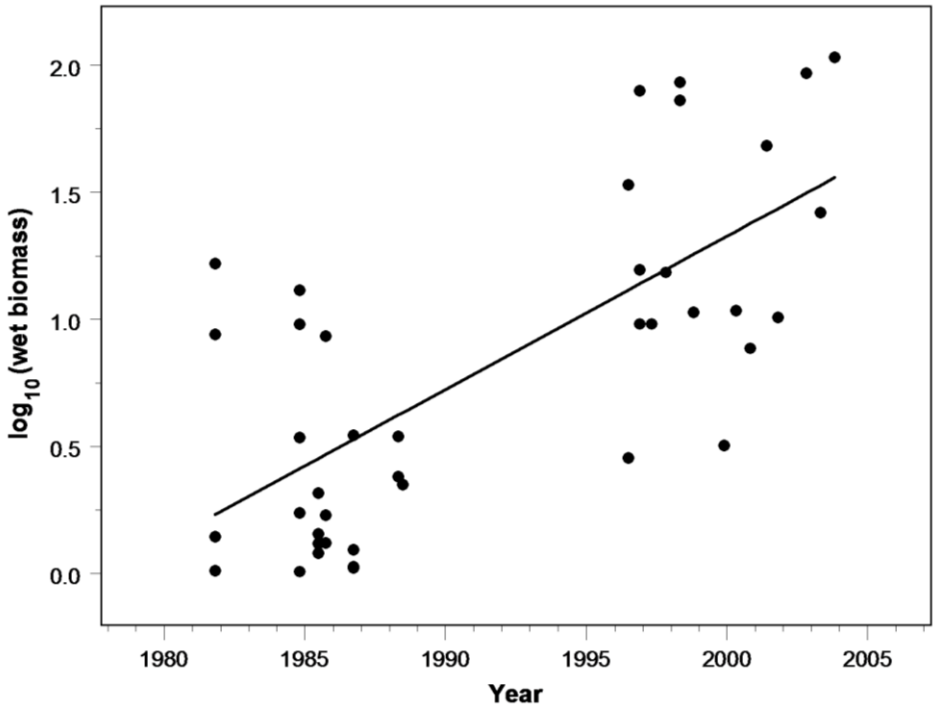

Figure 7. Mean Emerald Basin euphausiid column wet biomass vs. time from BIONESS sampling. Line is a least-squares linear regression fit to log biomass.

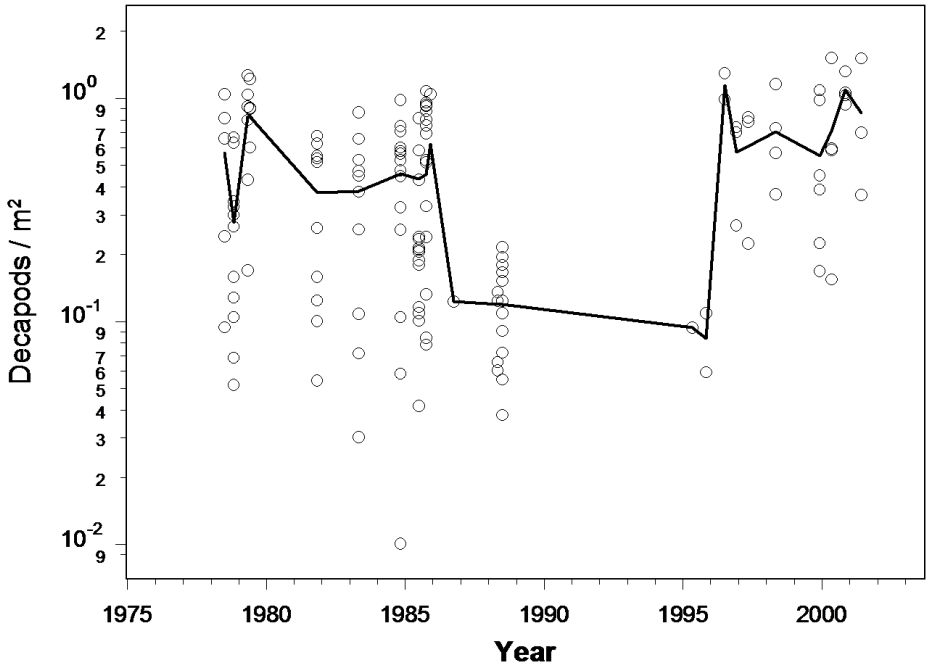

Figure 8. Mean column number of decapods vs. time collected with the BIONESS on the Scotian Shelf. The line is a least-squares fitted Kernel smoother.

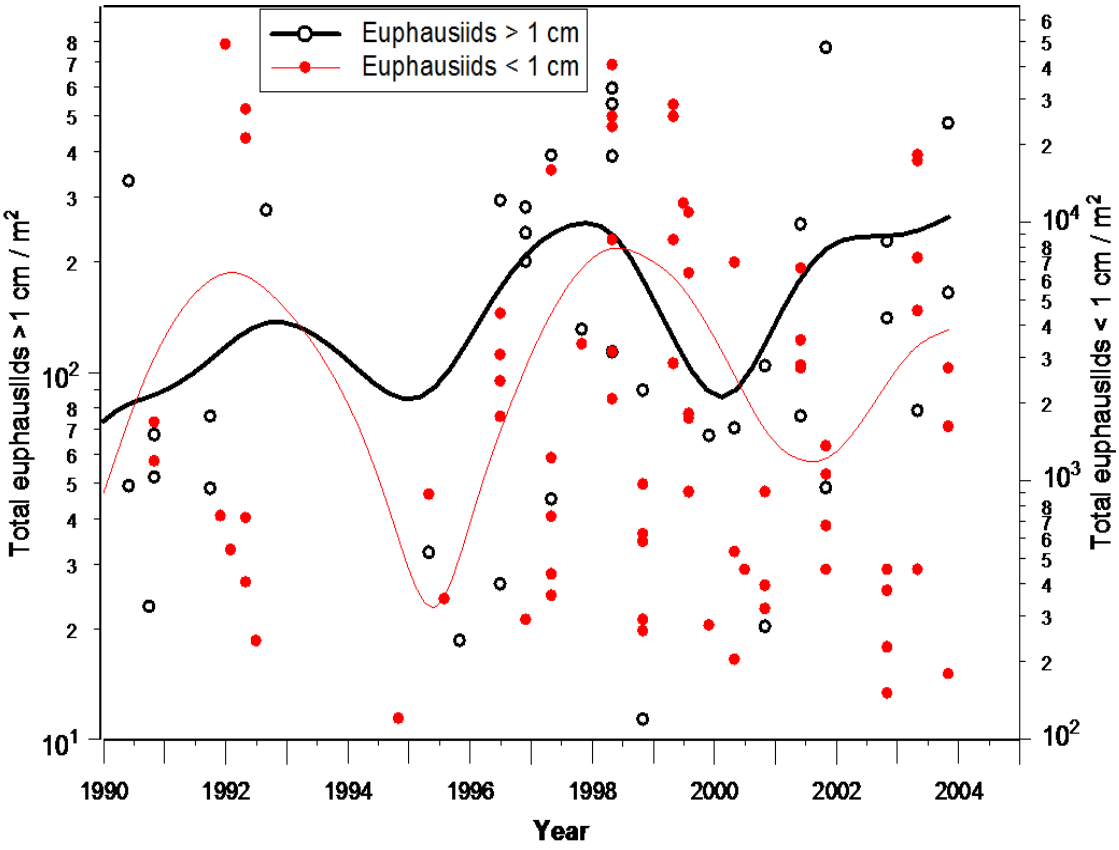

Figure 9. Mean column numbers of euphausiids > 1 cm length and of euphausiids < 1 cm length vs. time on the Scotian Shelf. The lines are least-squares fitted cubic spline smoothers. Note differing log scales for the two size components.

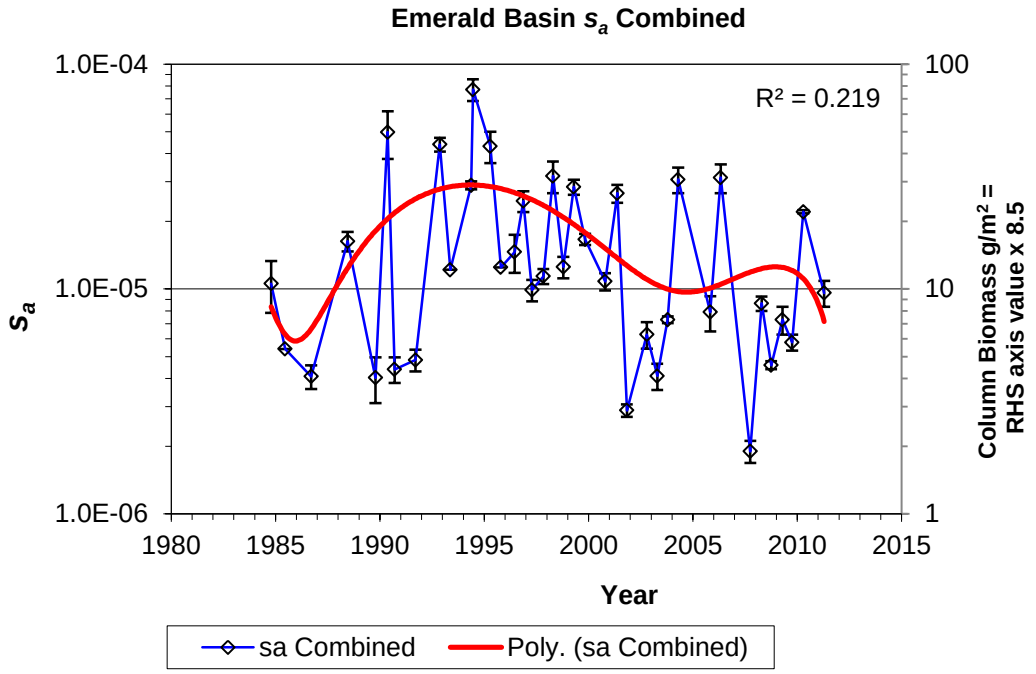

Figure 10. Mean column backscatter (s_a) vs. time for Emerald Basin using 200 kHz sounder, all surveys included. BIONESS and BATFISH type transects have been combined with S.E. error bars shown. A 5th order polynomial fit is shown in red.

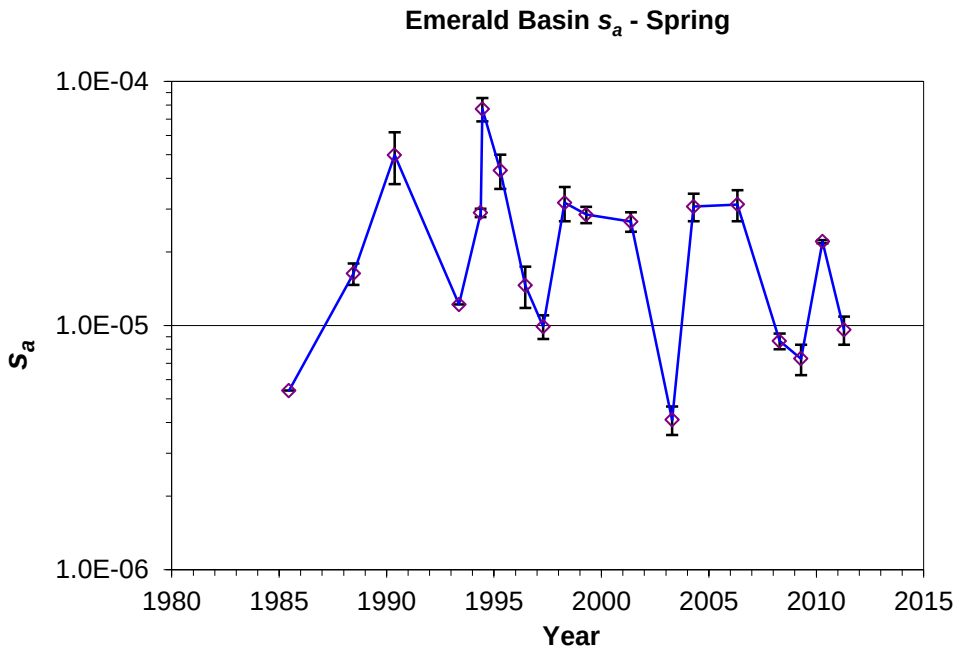

Figure 11. Mean column backscatter (s_a) vs. time for Emerald Basin using 200 kHz sounder during *spring* surveys. BIONESS and BATFISH type transects have been combined with S.E. error bars shown.

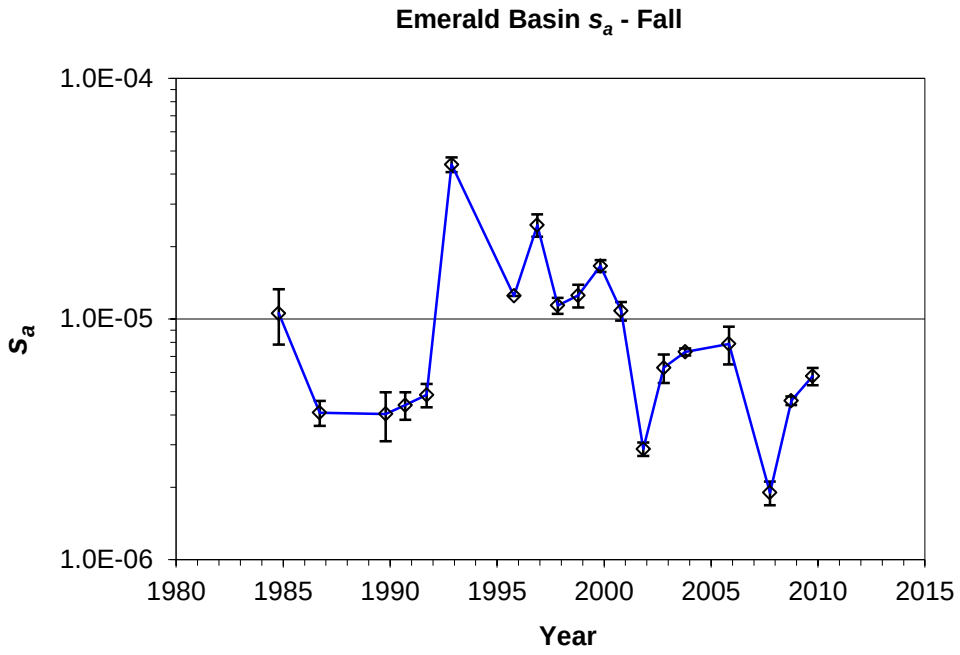

Figure 12. Mean column backscatter (s_a) vs. time for Emerald Basin using 200 kHz sounder during *fall* surveys. BIONESS and BATFISH type transects have been combined with S.E. error bars shown**.**

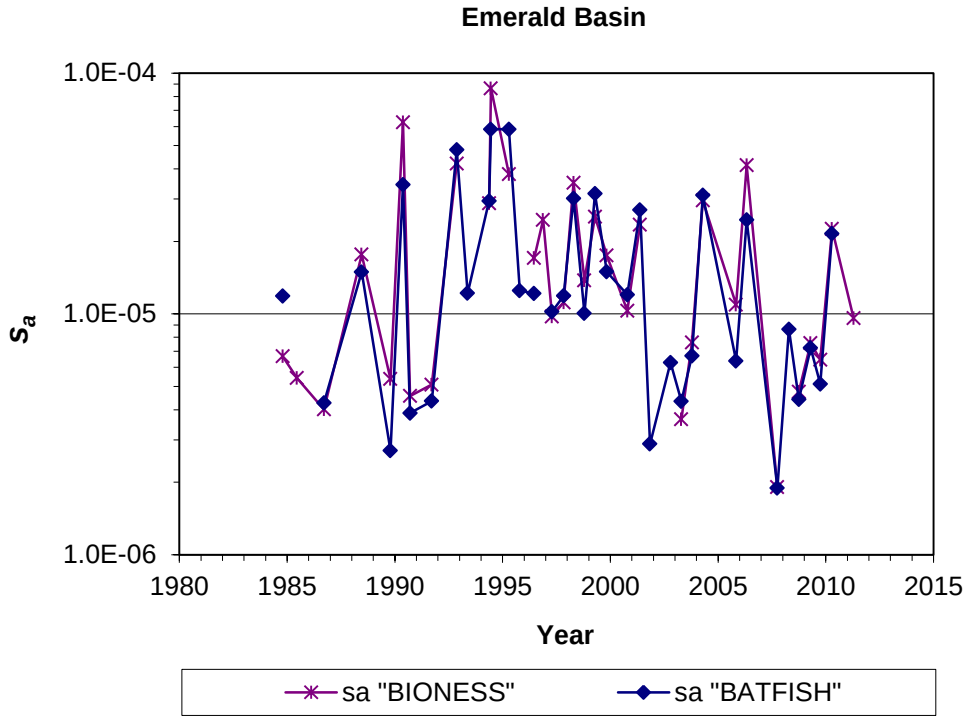

Figure 13. Mean column backscatter (s_a) vs. time for Emerald Basin using 200 kHz sounder during BATFISH (x) and BIONESS (♦) tows.

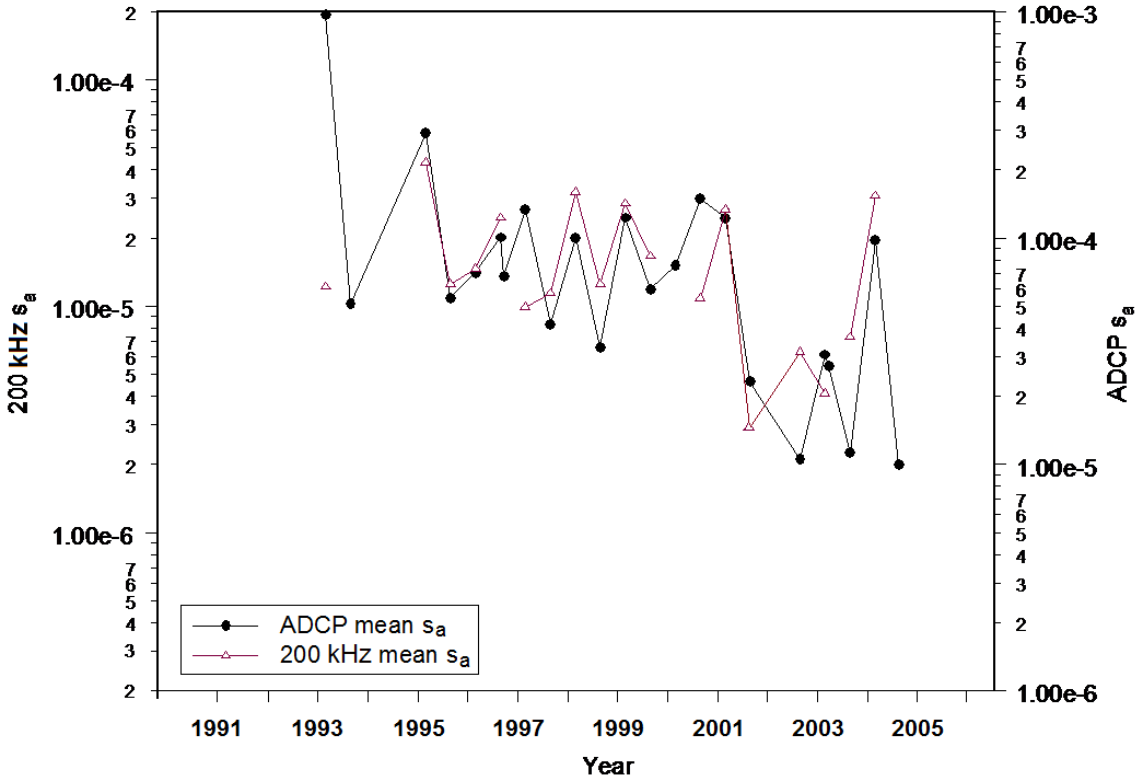

Figure 14. Mean column backscatter s_a vs. time for Emerald Basin using both the 200 kHz sounder and the ADCP.

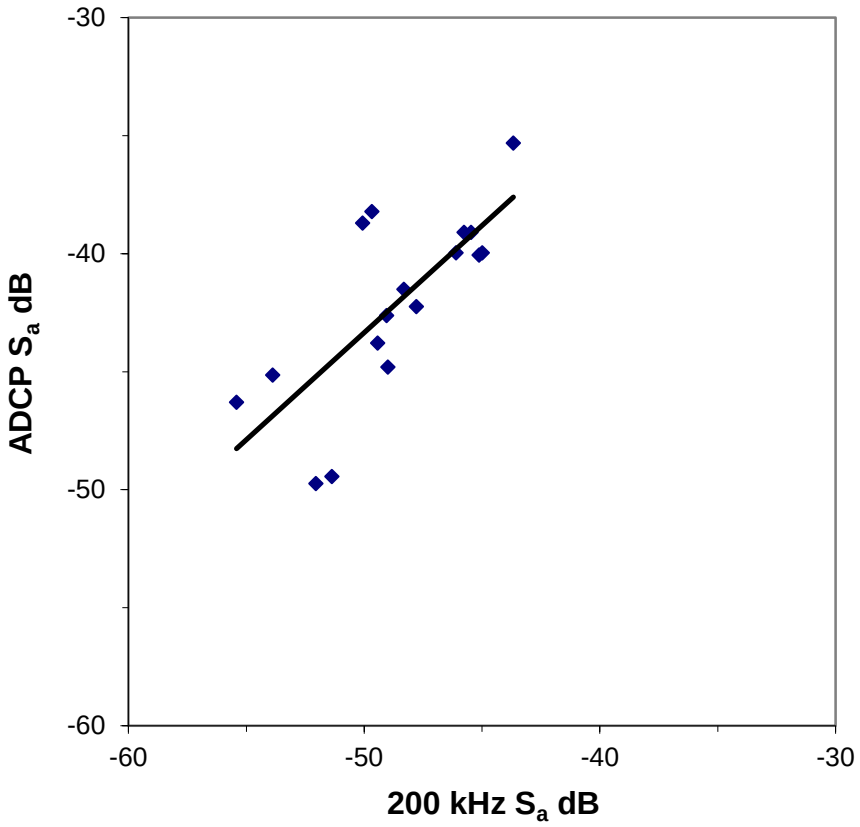

Figure 15. Least-squares linear regression between the ADCP and the 200 kHz sounder integrated backscatter (S_a) both expressed in decibel form as collected in Emerald Basin.

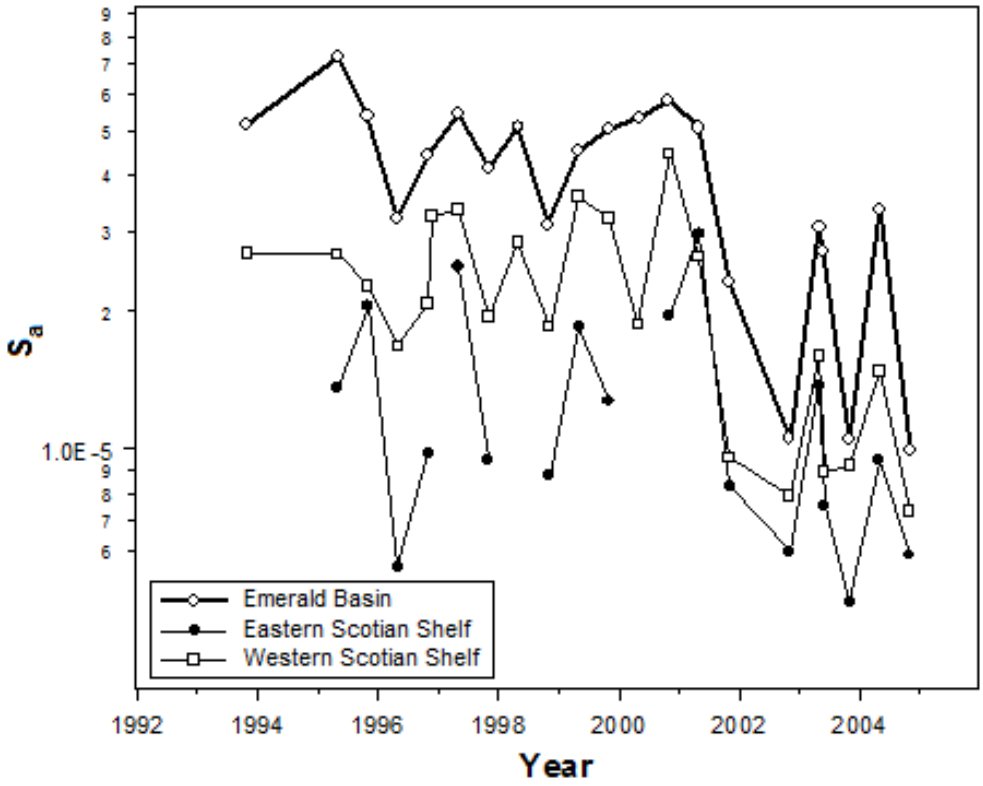

Figure 16. ADCP mean s_a values vs. time for the eastern and the western Scotian Shelf and for Emerald Basin.

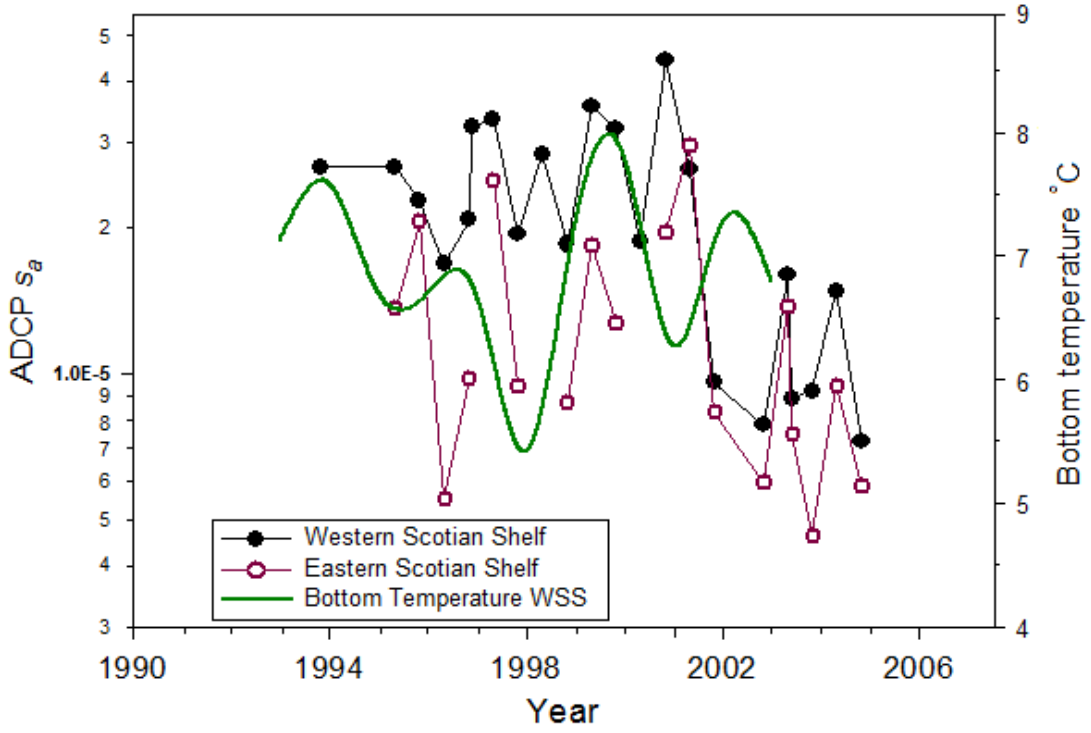

Figure 17. ADCP s_a mean values for the eastern and western Scotian Shelf and mean shelf bottom temperature vs. time.

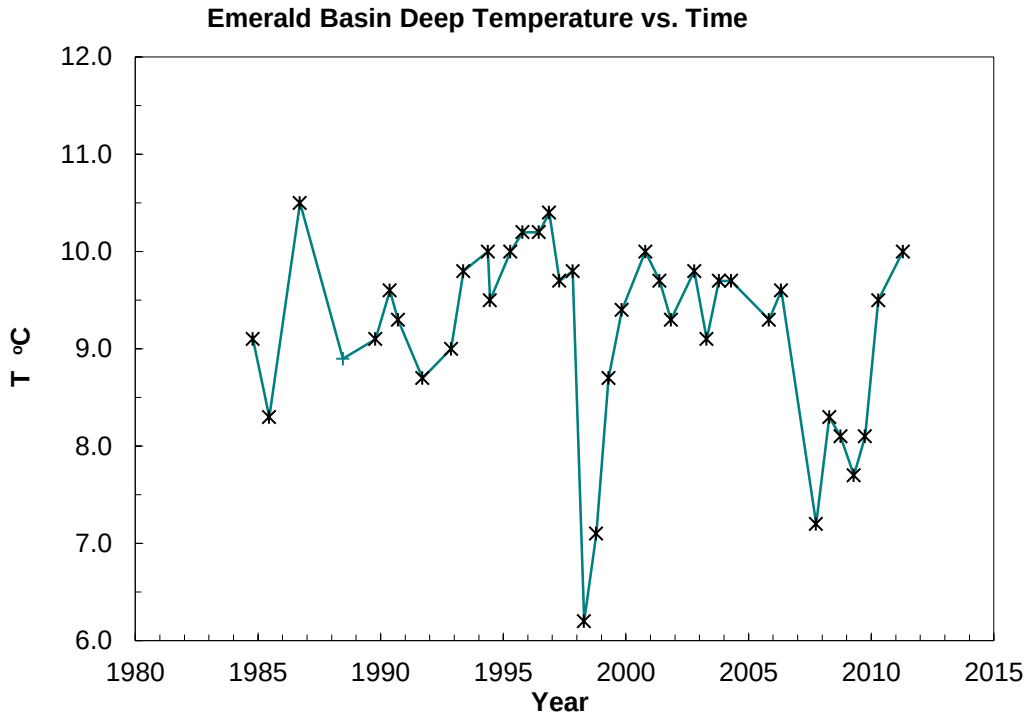

Figure 18. Emerald Basin near-bottom temperature vs. time.

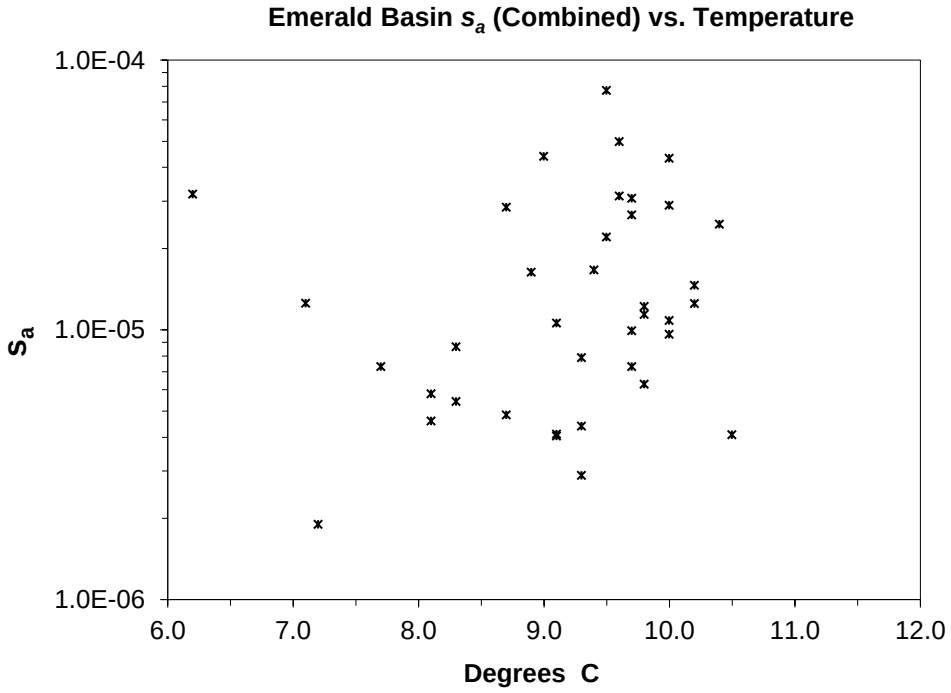

Figure 19. Emerald Basin 200 kHz column backscatter (s_a) vs. near-bottom temperature.

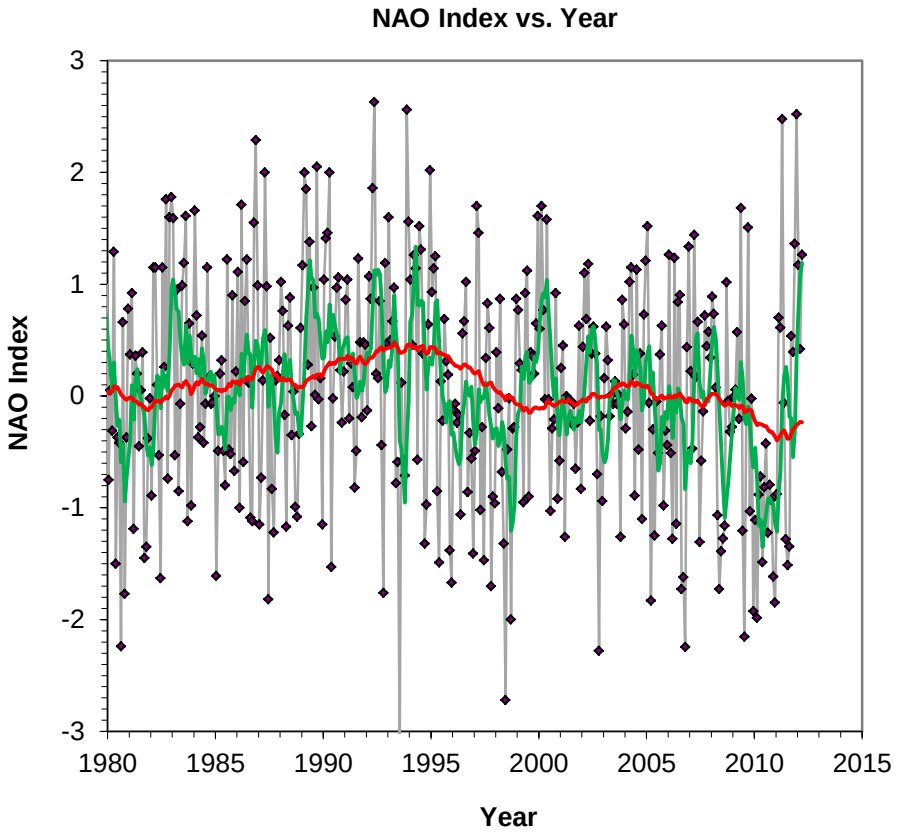

Figure 20. Monthly NAO index over primary study period. 1-year (green) and 5-year (red) causal running means (i.e. means plotted at end of averaging period) are superimposed.